

NRL Report 8425

**Ocean Environmental Influences of Temperature
and Mechanical Stress on Bare Fiber-Optic
Sensors of Acoustic Pressures
Part II**

S. HANISH

Acoustics Division

January 21, 1981



NAVAL RESEARCH LABORATORY
Washington, D.C.

Approved for public release; distribution unlimited.

REPORT DOCUMENTATION PAGE		READ INSTRUCTIONS BEFORE COMPLETING FORM
1. REPORT NUMBER NRL Report 8425	2. GOVT ACCESSION NO.	3. RECIPIENT'S CATALOG NUMBER
4. TITLE (and Subtitle) OCEAN ENVIRONMENTAL INFLUENCES OF TEMPERATURE AND MECHANICAL STRESS ON BARE FIBER-OPTIC SENSORS OF ACOUSTIC PRESSURES, PART II	5. TYPE OF REPORT & PERIOD COVERED Final report on one phase of the NRL problem	
	6. PERFORMING ORG. REPORT NUMBER	
7. AUTHOR(s) Sam Hanish	8. CONTRACT OR GRANT NUMBER(s)	
9. PERFORMING ORGANIZATION NAME AND ADDRESS Naval Research Laboratory Washington, D.C. 20375	10. PROGRAM ELEMENT, PROJECT, TASK AREA & WORK UNIT NUMBERS Program Element 62711N Project ZF11-121-004 J.O. 68136-6020 NRL Problem 81-F100-0-0	
11. CONTROLLING OFFICE NAME AND ADDRESS Defense Advanced Research Projects Agency 1400 Wilson Boulevard Arlington, VA 22209	12. REPORT DATE January 21, 1981	
	13. NUMBER OF PAGES 47	
14. MONITORING AGENCY NAME & ADDRESS (if different from Controlling Office)	15. SECURITY CLASS. (of this report) Unclassified	
	15a. DECLASSIFICATION/DOWNGRADING SCHEDULE	
16. DISTRIBUTION STATEMENT (of this Report) Approved for public release; distribution unlimited.		
17. DISTRIBUTION STATEMENT (of the abstract entered in Block 20, if different from Report)		
18. SUPPLEMENTARY NOTES		
19. KEY WORDS (Continue on reverse side if necessary and identify by block number) Fiber-optic sensor Fiber-optic hydrophone Temperature and stress dependence of fiber-optic hydrophones		
20. ABSTRACT (Continue on reverse side if necessary and identify by block number) Part I: A theoretical analysis is made of the signal-to-noise ratio of a fiber-optic hydrophone based on general forms of power spectra of random environmental noise. The signal is a single-frequency acoustic pressure wave. The noise is a sum of shot noise, laser jitter, environmental temperature fluctuations and environmental mechanical-stress fluctuations. Environmental effects are discussed in terms of autocorrelation functions and power spectra. Explicit formulas are derived for the case of Gaussian autocorrelations. <div style="text-align: right;">(Continued)</div>		

20. Abstract (Continued)

A detailed investigation is undertaken of the effects of temperature fluctuations in the ocean on the phase stability of the signal beam. Both large-scale temperature fluctuations caused by internal waves and small-scale fluctuations caused by velocity turbulence and thermal diffusion are considered. Numerical calculations are made of specific cases of interest. It is concluded that the stability of phase is either strongly affected or moderately affected, depending on the length of the fiber exposed to the medium, the depth in the ocean, the track length of towed sensors, the time of exposure in moored sensors, and the characteristics of built-in instrumental spectral windows.

Part II:

The effect of extraneous (environmental) mechanical stress on the state of polarization of light signals in fiber-optic sensors of acoustic pressure is investigated. After review of the relevant theory of the propagation of polarized light in a dielectric waveguide and of photo-elastic coupling, more specific cases of the birefringent effects of mechanical stress are theoretically analyzed and numerically calculated. It is concluded that these effects are negligible in the cases treated except for fibers subject to equal and opposite forces along a diameter or subject to random pressure fluctuations. Estimates of differential changes in the index of refraction in silica fibers due to (elastic) stress-induced birefringence are furnished.

CONTENTS

SUMMARY	iv
INTRODUCTION	1
CHARACTERIZATION OF THE STATE OF POLARIZATION OF LIGHT	2
TYPES OF BIREFRINGENT MEDIA	5
EVOLUTION OF THE STATE OF POLARIZATION WITH DISTANCE OF PENETRATION	6
EFFECTS OF DIELECTRIC POLARIZATION ON THE PROPAGATION OF LIGHT IN A WAVEGUIDE	7
Field Equations	7
Mode Coupling in a Dielectric Waveguide	9
Dielectric Polarization by Torsional Stress	11
Mode Coupling Coefficients for Pure Torsion	12
Evolution of Electric Vector Polarization in the Case of Pure Torsion of a Fiber	15
Periodic Dielectric Polarization	17
ANALYSIS BY PHOTOELASTICITY OF ELECTRIC FIELD POLARIZATION OF SINGLE MODE FIBERS UNDER MECHANICAL STRESS	17
Stress Analysis	18
Propagation of Polarized Light in Doubly Refracting Materials	18
Polarization Effects in Stressed Elastic Bodies	19
Summary	22
APPLICATIONS	22
NUMERICAL CALCULATIONS	34
Stress-Optic Constant C	34
Numerical Calculations of Fiber on a Mandrel (Case 6)	36
Bare Core on a Mandrel (Case 6)	38
Parameter Variation for Calculations of Δn of a Bare Core on a Mandrel (Case 6)	38
Fiber Squeezed by Diametral Press (Case 8)	39
Average Δn Along a Horizontal Diameter (Case 8)	39
Pure Torsion (Case 9)	40
Fiber Subject to Random Stresses (Case 8)	41
CONCLUSIONS	41
REFERENCES	42

SUMMARY

Polarized laser light conducted in optical fibers is modulated by time-varying and space-varying mechanical stress. Stress effects on states of polarization are particularly important in applications of optical fibers to sensing of acoustic and mechanical fields. Quantitative estimates are essential in these cases. The procedure for making these estimates followed these steps: first, to lay a firm groundwork for making numerical calculations a detailed review of the theory of coupling between electric fields and mechanical stress was undertaken. An important distinction was made between single-mode fibers carrying one mode and the same fibers carrying two degenerate modes. The results of this review are presented in a group of equations which are applied to the case of pure torsion. The resultant calculations agree with the work of Ulrich and Simon. Upon completion of this review a number of specific cases were calculated of the change in phase and state of polarization of polarized light in optical fibers disturbed by mechanical stress; these cases were

- Case 1. Applied stress on the fiber is axisymmetric and everywhere uniform along the optical path
- Case 2. Applied stress on the fiber is axisymmetric but varies along the optic path
- Case 3. Tensile or compressive stresses are applied to the ends of the fiber
- Case 4. Oblique incidence of optic ray and pure bending
- Case 5. Fiber subject to both bending and shear
- Case 6. Fiber wrapped on a mandrel
- Case 7. Fiber subject to random stress
- Case 8. Fiber squeezed by diametral forces
- Case 9. Pure torsion

It is concluded that the birefringent effects are negligible in most applications because there are no components of stress transverse to the optic ray. Two important cases do show birefringent effects, fiber squeezed by diametral forces and fiber subjected to random stresses. Numerical calculations predict that for fibers of fused silica, at the limit of allowable stress,

$$\Delta n_{\max} = -8.5 \times 10^{-4} \text{ for the case of applied diametral forces}$$

and

$$\Delta \phi_d \approx 1 \text{ rad if the rms stress fluctuation is } 23.4 \text{ kPa (3.4 psi).}$$

The case of a fiber 80 μm in diameter with a core 4.5 μm in diameter wound on a mandrel 1 cm in diameter has also been numerically estimated for fused silica at the maximum allowable stress. Here the birefringent effect is negligible if the optic ray is parallel to the axis of the fiber. However, if the optic ray is incident at 4° to the optic fiber axis, then it is estimated that

$$\Delta n_{\max} \approx -2.5 \times 10^{-4}.$$

OCEAN ENVIRONMENTAL INFLUENCES OF TEMPERATURE AND MECHANICAL STRESS ON BARE FIBER-OPTIC SENSORS OF ACOUSTIC PRESSURES PART II

INTRODUCTION

The effect of an optical waveguide fiber under various conditions of temperature, pressure, etc. upon the state of polarization of incident light has been investigated by several authors [1-3]. Recently, these studies have been made in connection with the magneto-optic (Faraday) effect [4,5]. Although varied in details, most papers present the typical laboratory experimental setup of Fig. 1: A He-Ne laser (1) generates linearly polarized light with a fixed plane of polarization. This passes through a quarter-wave plate (2) and emerges circularly polarized. The light then enters a polarizer (a Glan-Thompson prism) (3), which is mounted on a rotatable fixture, and emerges linearly polarized at any desired polarizing angle. This beam is then focused by a microscope objective (4) onto a fiber (5). A watertight compartment (6) allows measurement at various fiber temperatures. The emerging light is collimated by a lens (7) and then analyzed by a rotatable Wollaston prism (8), which splits the incident light into slow and fast components by birefringence (9). These components are detected by photodetectors (10) which deliver intensities I_1 and I_2 .

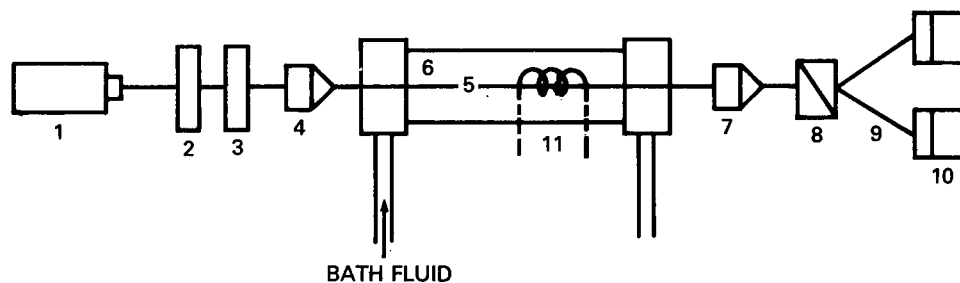


Fig. 1 — Experimental study of polarization

During the experiment the polarizer (2) is set to an arbitrary angle Φ (input polarization angle) and the analyzer (8) is rotated to an output angle ψ such that one of the emerging beams has a maximum intensity I_{\max} and the other has a minimum intensity I_{\min} . The degree of polarization P is then determined by analog electronic circuits,

$$P = \frac{I_{\max} - I_{\min}}{I_{\max} + I_{\min}}$$

Thus polarization effects of a fiber of length L are characterized by measurement of Φ , ψ , and P as a function of environment (temperature, pressure, etc.). A birefringent model of the fiber then relates L

to the phase difference δ between fast and slow modes. In this way δ is deduced by measurement. The magneto-optic effect on polarization is studied by introducing a magnetic field with a coil (11).

In applications of optical waveguides to such tasks as communications, measurement, and control of information and processes the concept of *depolarization* is crucial. This refers to reduction in P and change (possible randomization) in ψ and δ due to temperature and mechanical stress. It also refers to the loss of coherence between fast and slow waves in the fiber caused by the same external factors. A summary of facts and theories of partially polarized light is found in standard treatises [6, p. 552].

This report will concentrate on the theory of the effect of mechanical stress or strain on the state of polarization of a light beam in an optical waveguide fiber. An experimental setup to study this effect could be the same as in Fig. 1 except for replacement of the temperature-controlled bath by various strain-induced deformations of the fiber.

CHARACTERIZATION OF THE STATE OF POLARIZATION OF LIGHT

A brief review of standard theory will help clarify more advanced concepts in this report. The propagation of polarized light $\mathbf{E} = (E_x, E_y, E_z)e^{i\omega t}$ in a fiber can be visualized as the trace of the tip of the vibrating electric vector transverse to the direction of propagation. In general this trace is a helix whose radius varies with distance of propagation. The projection of an adjacent portion of the helix on any transverse plane is an ellipse whose semimajor axis is a units long, oriented at angle ψ relative to the x axis, and whose semiminor axis is b units long. The helix is called right handed (or positive) if an observer looking face on at the source of light sees the electric vector rotating clockwise; it is left handed (or negative) if the vector is rotating anticlockwise. A reversal in direction of the ellipse means a switch from positive to negative, that is, the azimuth angle χ changes by π radians. To any ellipse with its major axis at azimuth α there corresponds an *orthogonal ellipse* whose major axis is at $90^\circ + \alpha$. Since the ellipse can be represented in parametric (or component) form,

$$E_x = a \cos (\tau + \delta_1)$$

and

$$E_y = b \cos (\tau + \delta_2),$$

or

$$\frac{E_y}{E_x} = \frac{b}{a} e^{-i(\delta_1 - \delta_2)},$$

its orientation (angle ψ) depends on $\delta_1 - \delta_2$. When the phase δ changes with distance of travel z , its magnitude at wavenumber k is

$$\delta = kz = k_0 nz = \frac{2\pi}{\lambda_0} nz,$$

where n is the index of refraction and λ_0 is the wavelength of the light. Thus,

$$\delta_1 - \delta_2 = \frac{2\pi}{\lambda_0} z (n_1 - n_2).$$

In an anisotropic (birefringent) fiber $n_1 \neq n_2$. This causes the ellipse to change orientation as it propagates.

A positive (clockwise) ellipse at fixed azimuth χ ranges in appearance from a line ($b = 0$) to an ellipse ($b \neq a$) to a circle ($b = a$). A negative ellipse exhibits the same series of shapes, except with reversed rotation.

The variation of the components E_x , E_y , E_z propagating in an optical fiber along coordinate z can be studied by the matrix algebra of the Jones calculus [7]. An equally illuminating procedure is to model the state of polarization of the light as a point on the surface of a unit (Poincaré) sphere S [8]. On this sphere an *arbitrary* point represents a state of elliptic polarization which is traced out in time by the electric vector at a particular cross section $z = \text{const.}$ of the fiber. All latitudes above the equator represent positive rotation; those below represent negative rotation. Since the relative shape of the ellipse can be given by the ratio b/a of its axes, and its orientation by an angle ψ of the major axis relative to some reference line, the point on S can be located by two angles: an azimuth angle 2ψ , and an elevation angle 2χ (Fig. 2). The angle appears double because an ellipse completes a cycle of orientation in a plane cross section in π radians (180°), whereas a point P completes the same cycle on S in 2π radians (360°). Also, since χ varies from 0 to 45° as b/a varies from 0 to 1 , it is seen that

$$\tan \chi = b/a.$$

Two special cases of the elliptical state of polarization appear on S .

Ellipse degenerates to a line ($b = 0$)

Here $\chi = 0$, hence, all polarization states P are found on the equator (Fig. 2). At point H the angle $2\psi = 0$; the light is then linearly polarized in the direction of the x axis. At point V the angle $2\psi = \pi$, or $\psi = 90^\circ$; the light is then linearly polarized in the direction of the y axis. At C the plane of polarization is 45° relative to the x axis, and at D it is 135° .

Ellipse degenerates to a circle ($b/a = 1$)

Here $\tan \chi = 1$ (i.e., $2\chi = 90^\circ$). There are only two states of polarization, L and R (Fig. 2). Point L (north pole) represents circularly polarized light rotating counterclockwise (when looking from L toward the origin), while point R (south pole) represents circularly polarized light rotating clockwise (when looking from R toward the origin).

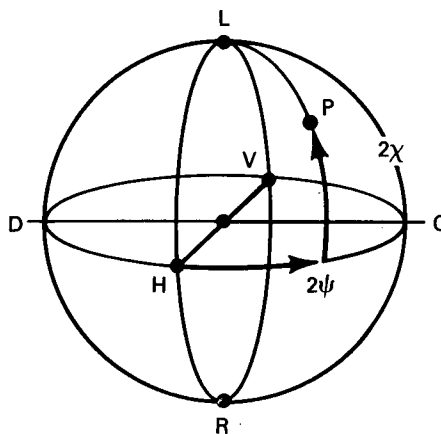


Fig. 2 — Angles 2ψ and 2χ on a Poincaré sphere

When a light beam of specified polarization (P_1 on S) enters a birefringent medium, its state P_2 at increment dz of penetration is a point on the trajectory $dC(z)/dz$ of the unit radius vector $C(z)$ on S whose initial terminus is P_1 . This change from P_1 to P_2 is caused by the phase advance δ with distance of penetration of the fast component of the light vector over the slow component, which thus alters the initial time phase of the light vector components along the major and minor axes of the ellipse at P_1 . Since any incremental trajectory on the surface of a sphere corresponds to a rotation about some diameter, one can find state P_2 by rotating the entire sphere S through an angle δ about a uniquely chosen axis of rotation AA_a , where A and A_a are opposite points at the ends of a single diameter, representing the two *unique* polarization states (or eigenstates) of the medium relative to some reference line.

For example, assume that a linear birefringent medium is so oriented that it resolves an incident linearly polarized light into two linearly polarized orthogonal components, one along X and the other along Y . Directions X and Y are taken to be the privileged axes along which the *states* of polarization do not change with penetration. The component along X is at state H on S , while the component along Y is at state V . The axis HV is therefore the axis of rotation for any state P_1 moving along trajectory $C(z)$ to state P_2 . To illustrate, let P_1 be a linearly polarized beam incident on the birefringent medium at $\theta_0 = 20^\circ$ relative to X . Its point on S is on the equator at azimuth angle 40° relative to HV . It is resolved by the medium along the privileged axes X and Y , where the resultant components travel at different speeds. After the beam penetrates a distance ΔZ , the phase along the fast axis (say H) advances (say) $\delta = 15^\circ$ ahead of the phase along the slow axis (say V). The state P_2 (ΔZ) on S is then obtained by rotating the entire sphere about HV counterclockwise (looking from the fast axis H toward the origin) through an angle of 15° (Fig. 3). Since the elevation angle 2χ of P_2 is different from zero, it is seen that state P_2 represents elliptical polarization,

$$\begin{pmatrix} E_x \\ E_y \end{pmatrix} = \begin{bmatrix} e^{j\delta/2} & 0 \\ 0 & e^{-j\delta/2} \end{bmatrix} \begin{pmatrix} \cos\theta_0 \\ \sin\theta_0 \end{pmatrix} E_0 e^{j\omega t}.$$

The angle ψ of the major axis satisfies the equation

$$\tan 2\psi = \tan 2\theta_0 \cos\delta = \tan 40^\circ \cos 15^\circ = 0.81,$$

or $2\psi = 39.02^\circ$ and $\psi = 19.51^\circ$. The relations between E_{\max} , E_{\min} , E_y , E_x , E_0 , ψ , and θ_0 are shown in Fig. 4. The new coordinates of polarization state P_2 are azimuth angles $2\psi_2$ and elevation angles $2\chi_2$.

In sum, in this example the incident wave, linearly polarized at $\theta_0 = 20^\circ$, becomes elliptically polarized at 19° . The magnitudes of E_{\max} , E_{\min} , and degree of polarization will be discussed later.

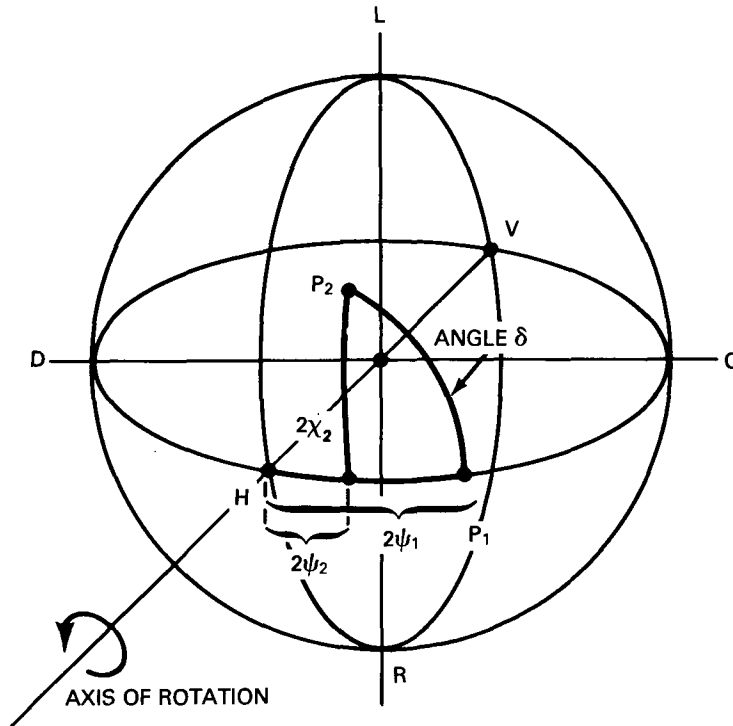


Fig. 3 — Evolution of state of polarization from P_1 to P_2

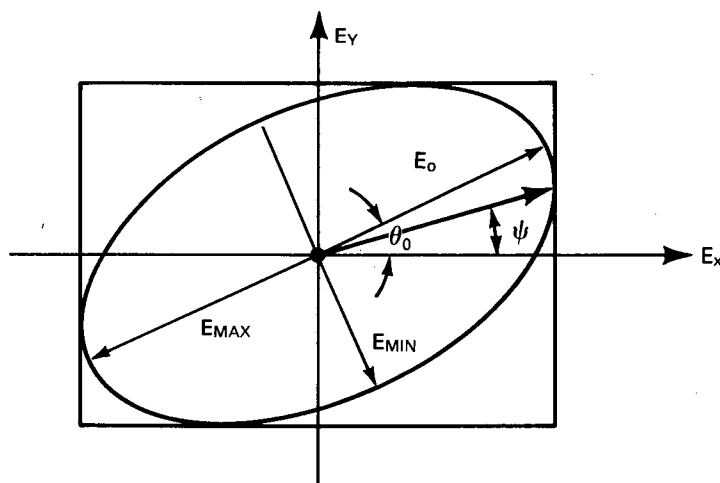


Fig. 4 — Definitions of parameters in elliptical polarization

TYPES OF BIREFRINGENT MEDIA

The axis of rotation AA_a on the Poincaré sphere is determined by the optical properties of the medium. Three types of media can be described.

A medium which has two eigenstates of linear polarization is called a linear birefringent medium. When a beam with elliptical polarization is incident on this type, it is resolved into two orthogonal linearly polarized beams (referred to as the fast beam and the slow beam). In this medium all axes of rotation are diameters confined to the equatorial plane of the S sphere. The unique diameter (axis of rotation) for a given state P_1 is fixed by the orientation of the privileged birefringent axes relative to the X and Y axes of the (transverse) coordinate system. In the above example the unique diameter was HV . The direction of rotation is always taken to be counterclockwise around the faster state when looking toward the origin.

A medium which has two eigenstates of circular polarization is called a circular birefringent medium. When a beam with elliptic polarization is incident on this type of medium, it is resolved into two circularly polarized beams of opposite rotation. The unique diameter of rotation is the axis LR on the S sphere. The trajectory of new states $P_2(\Delta Z)$ lies on latitude circles, and the direction of rotation is counterclockwise about the faster state, as in the previous case. When the incident-beam polarization is linear, this medium resolves the beam into two oppositely rotating, equal-amplitude, circularly polarized beams. The net effect after the beam penetrates a distance ΔZ is rotation of the incident plane of polarization to a new plane. This medium exhibits optical activity.

A medium which has two eigenstates of elliptical polarization is called an elliptically birefringent medium. When a beam with elliptic polarization is incident on this type of medium, it is resolved into two elliptically polarized beams with opposite rotation. The unique axis of rotation for a given state P_1 is an arbitrary diameter of the S sphere. This medium exhibits a combination of birefringence and optical activity. The incremental rotation Δ' due to an incremental birefringent phase difference δ' and an incremental optical activity ρ' is

$$\Delta' = \sqrt{\delta'^2 + (2\rho')^2}.$$

The unique axis of rotation for a state P_1 is a diameter lying in the plane of the corresponding linearly birefringent medium axis, but at an elevation such that

$$2\chi = \arctan \frac{2\rho'}{\delta'}.$$

The direction of rotation is counterclockwise about the faster state.

EVOLUTION OF THE STATE OF POLARIZATION WITH DISTANCE OF PENETRATION

Ulrich and Simon [9] have studied the effect of twist on the state of polarization of single-mode fibers. Their approach is reviewed here.

Let $\omega(z)$ be a vector in xyz space whose magnitude $|\omega|$ is chosen to represent the angle of rotation per unit length of penetration and whose associated spherical angles $2\chi_\omega$ and $2\xi_\omega$ locate the end point of a diameter of an S sphere which forms the axis of rotation. Let $C(z)$ be a unit vector of this sphere extending from the origin of S to the state-of-polarization point P_1 at distance Z along the fiber. Then the new state of polarization a short distance beyond Z is given by

$$\frac{dC(z)}{dz} = \omega(z) \times C(z).$$

Assume that state P_1 represents elliptical polarization and assume that the medium rotates P_1 through an angle $\beta(z)$ due to birefringence and an angle $\alpha(z)$ due to optical activity. Then the total rotation vector for small increments in C is

$$\omega(z) = \alpha(z) + \beta(z).$$

First, let ω , α , and β be independent of z . There are then two points ($\pm \omega/\omega$), at the ends of a fixed diameter on a Poincaré sphere, which are the privileged directions of propagation of the two eigenstates of elliptic polarization. In the cross section ($z = \text{const.}$) of an optical fiber the orientation of these ellipses is given by β (a constant). The length ratio of the axes is given by the elevation angle 2χ , where (as before)

$$\tan \chi = \frac{|\alpha|}{|\beta|}.$$

Next, let α and β depend on travel distance z . This is the case of a twisted birefringent fiber. As the polarized light penetrates the fiber, two events occur simultaneously: (a) the privileged axes of birefringence rotate and (b) the phase of the fast wave relative to the slow wave increases. Both effects can be modeled. To model event (b), Ulrich and Simon [9] insert a local Cartesian coordinate system R^0 at each $z = z^0$, and orient x^0 and y^0 to be parallel to the local fast and slow axes respectively. Polarization changes in this local system are represented on the S^0 sphere by the unit vector C_Ω^0 rotating about the axis of rotation Ω^0 fixed in S^0 . To determine the magnitude and direction of Ω^0 , one must be given the birefringence rotation β^0 , the optical activity rotation α^0 , and the angle of twist rotation τ^0 , all in R^0 . Then

$$\Omega^0 = \beta^0 + \alpha^0 - 2\tau^0.$$

The factor 2 appears here because azimuths on a Poincaré sphere are twice those of real space. The minus sign is a convention that the twist is clockwise as z advances while the rotations β^0 and α^0 are counterclockwise. In the local system diameter Ω^0 defines two eigenstates of elliptical polarization $\pm \Omega^0/\Omega$ which propagate in R^0 unchanged.

To model event (a), the entire local S^0 is rotated about LR at a rate 2τ relative to fixed laboratory coordinates. Thus the total trajectory $C(z)$ of the polarization state is the vector sum of a trajectory

along the rim of the base of a cone on S^0 (apex at the origin) plus the trajectory imparted by the generator of the cone as its tip moves in a latitude circle around RL of the laboratory-fixed sphere S . The combination makes $C(z)$ trace out a cycloid on S .

This analysis closely parallels that of the general motion of a spinning top in which Ω^0 is the analog of the angular velocity of the top in a local coordinate system, and τ is the angular velocity of the local system relative to the fixed laboratory system. The top undergoes precession, which is the analog of the birefringent effect alone, and nutation, which is the analog of the combination of optical activity and birefringence.

The trajectories described above depend on specifically located axes of rotation. The determination of these axes is sufficiently complicated in the general case to require a complete review of the theory of the effects of perturbations of the dielectric polarization on the propagation of light in a dielectric waveguide. This is taken up next.

EFFECTS OF DIELECTRIC POLARIZATION ON THE PROPAGATION OF LIGHT IN A WAVEGUIDE

Field Equations

Maxwell's equations in the SI units form the starting point for this analysis:

$$\nabla \times \mathbf{H} = \mathbf{J} + \frac{\partial \mathbf{D}}{\partial t}, \quad (1)$$

$$\nabla \times \mathbf{E} + \frac{\partial \mathbf{B}}{\partial t} = 0, \quad (2)$$

$$\nabla \cdot \mathbf{D} = \rho, \quad (3)$$

and

$$\nabla \cdot \mathbf{B} = 0, \quad (4)$$

where the units are \mathbf{H} , $\text{A}\cdot\text{m}^{-1}$; \mathbf{J} , $\text{A}\cdot\text{m}^{-2}$; \mathbf{D} , $\text{C}\cdot\text{m}^{-2}$; \mathbf{E} , $\text{V}\cdot\text{m}^{-1}$; ρ , $\text{C}\cdot\text{m}^{-3}$; and \mathbf{B} , $\text{V}\cdot\text{s}\cdot\text{m}^{-2}$.

To this set one adds the constitutive equations which relate \mathbf{B} and \mathbf{H} and which relate \mathbf{D} and \mathbf{E} :

$$\mathbf{B} = \mu_0 \mathbf{H} + \mu_0 \mathbf{M} = \mu' \mathbf{H}, \quad \mu' = \mu_0 (1 + \mathbf{M}\mathbf{H}^{-1}) \quad (5)$$

and

$$\mathbf{D} = \epsilon_0 \mathbf{E} + \mathbf{P}, \quad (6)$$

where the units are μ , $\text{N}\cdot\text{s}^2/\text{C}^2$; ϵ , $\text{C}^2/\text{N}\cdot\text{m}^2$; \mathbf{M} , $\text{A}\cdot\text{m}^{-1}$; and \mathbf{P} , $\text{C}\cdot\text{m}^{-2}$. The vectors \mathbf{P} and \mathbf{M} are the dielectric polarization and magnetization respectively.

Assume $\mathbf{J} \equiv 0$. Elimination of \mathbf{B} from (1) and (2) leads to an equation in \mathbf{E} ,

$$\nabla^2 \mathbf{E} - \nabla(\nabla \cdot \mathbf{E}) - \mu' \epsilon_0 \frac{\partial^2 \mathbf{E}}{\partial t^2} - \mu' \frac{\partial^2 \mathbf{P}}{\partial t^2} = 0. \quad (7)$$

In this analysis we neglect magnetization and set $\mu' \approx \mu_0 = O(1)\text{Ns}^2\text{C}^{-2}$. Also, in the absence of true charge ρ the displacement \mathbf{D} is a constant. Thus,

$$\nabla \cdot \mathbf{D} = \nabla \cdot (\epsilon_0 \mathbf{E} + \mathbf{P}) = 0 \quad (8)$$

or

$$\nabla \cdot \mathbf{E} = -\epsilon_0^{-1} (\nabla \epsilon_0 \cdot \mathbf{E}) - \epsilon_0^{-1} \nabla \cdot \mathbf{P}.$$

We apply Eq. (7) to a fused silica waveguide of very small diameter. In the normal state of this material we assume \mathbf{P} to be negligible. In the perturbed state caused by mechanical, thermal, or optical stresses the vector \mathbf{P} takes on significant magnitudes. A simple model which is useful for our purposes has \mathbf{P} proportional to \mathbf{E} ,

$$\mathbf{P} = \mathbf{U}\mathbf{E}, \quad (9)$$

in which the SI units of the elements of dyadic \mathbf{U} are those of the dielectric constant ϵ , namely, $\text{C}^2/\text{m}^2 \cdot \text{N}$. Applying (8) and (9) in the steady state (frequency $f = \omega/2\pi$) to (7), one obtains

$$\nabla^2 \mathbf{E} + \nabla [\epsilon_0^{-1} \nabla \epsilon_0 \cdot \mathbf{E} + \epsilon_0^{-1} \nabla \cdot \mathbf{U}\mathbf{E}] + k^2 \mathbf{E} + \epsilon_0^{-1} k^2 (\mathbf{U}\mathbf{E}) = 0, \quad (10)$$

where

$$\mu' \omega^2 \epsilon_0 \approx \mu_0 \epsilon_0 \omega^2 \rightarrow k^2.$$

For high purity fibers we can readily assume that $\nabla \epsilon_0$ is negligible.

To apply Eq. (10) we must deal with components of vectors. A useful decomposition is, in tangential (superscript t) and longitudinal (superscript z) components,

$$\mathbf{E} = \mathbf{E}^t + \hat{k} E^z,$$

$$\nabla^2 = (\nabla^t)^2 + \frac{\partial^2}{\partial z^2},$$

$$\nabla^t = \hat{i} \frac{\partial}{\partial x} + \hat{j} \frac{\partial}{\partial y},$$

and

$$\mathbf{P} = \mathbf{P}^t + \hat{k} P^z = (\mathbf{U}\mathbf{E})^t + \hat{k} (\mathbf{U}\mathbf{E})^z.$$

In this report interest will be focused mainly on the tangential vector \mathbf{E}^t . Its propagation is governed by the reduced equation,

$$\nabla^2 \mathbf{E}^t + \nabla^t (\epsilon_0^{-1} \nabla \cdot \mathbf{U}\mathbf{E}) + k^2 \mathbf{E}^t + \epsilon_0^{-1} k^2 (\mathbf{U}\mathbf{E})^t = 0. \quad (11)$$

We seek a solution of (11) as a superposition of waveguide modes in a circular fiber,

$$\mathbf{E}^t(x, y, z) = \sum_m a_m(z) e^{ik_m z} \mathbf{E}_m^t(x, y) \quad (12a)$$

and

$$\mathbf{U}\mathbf{E}(x, y, z) = \sum_m a_m(z) (e^{ik_m z} \mathbf{U}\mathbf{E}_m)^t + \hat{k} (e^{ik_m z} \mathbf{U}\mathbf{E}_m)^z. \quad (12b)$$

Now

$$\nabla^2 \mathbf{E}^t = \sum_m a_m(z) e^{ik_m z} [(\nabla^t)^2 \mathbf{E}_m^t - k_m^2 \mathbf{E}_m^t] + \sum_m e^{ik_m z} [a_m'' + 2ik_m a_m'], \quad (13)$$

in which the prime in a_m' means $\partial/\partial z$. When (13) is inserted into (11) a number of terms of the latter cancel because they satisfy the steady-state wave equation of waveguide modes, in which the expansion coefficient $a_m(z) = a_m = \text{constant}$,

$$(\nabla^2)^2 \mathbf{E}_m^t + (k^2 - k_m^2) \mathbf{E}_m^t = 0. \quad (14)$$

We therefore consider only the second sum in Eq. (13). In it, all terms in $a_m''(z)$ are negligible for $z > \lambda$, $\lambda = 2\pi/k$. Thus the propagation of \mathbf{E}_m^t is governed by the equation

$$\begin{aligned} & \sum_m e^{ik_m z} \left\{ 2ik_m a_m'(z) (\hat{i}E_m^x + \hat{j}E_m^y) + a_m \epsilon_0^{-1} k^2 [\hat{i}(\mathbf{U}\mathbf{E}_m)^x + \hat{j}(\mathbf{U}\mathbf{E}_m)^y] \right. \\ & + a_m \epsilon_0^{-1} \left\{ \hat{i} \left[\frac{\partial^2}{\partial x^2} (\mathbf{U}\mathbf{E}_m)^x + \frac{\partial^2}{\partial x \partial y} (\mathbf{U}\mathbf{E}_m)^y \right] + \hat{j} \left[\frac{\partial^2}{\partial y \partial x} (\mathbf{U}\mathbf{E}_m)^x + \frac{\partial^2}{\partial y^2} (\mathbf{U}\mathbf{E}_m)^y \right] \right\} \\ & \left. + a_m \epsilon_0^{-1} \left[\hat{i} \frac{\partial^2}{\partial x \partial z} e^{ik_m z} (\mathbf{U}\mathbf{E}_m)^z + \hat{j} \frac{\partial^2}{\partial y \partial z} e^{ik_m z} (\mathbf{U}\mathbf{E}_m)^z \right] \right\} = 0. \end{aligned} \quad (15)$$

In this infinite sum one can find a_m' in terms of a_m by use of the orthogonality of modes in the waveguide. The relation a_m'/a_m determines the coupling of modes caused by the dielectric polarization. Its calculation is described next.

Mode Coupling in a Dielectric Waveguide

The time-averaged flux of energy in a waveguide is

$$W = \oint (\mathbf{E} \times \mathbf{H}^*) \cdot \hat{k} dA = \oint (\mathbf{E}^t \times \mathbf{H}^{**})^z dA. \quad (16)$$

For each mode,

$$W_m = \delta_{mn} \oint (\mathbf{E}_m^t \times \mathbf{H}_n^{**})^z dA. \quad (17)$$

We apply this formula to a circular fiber whose diameter is so small as to permit the propagation of a single mode only. Since this mode can be arbitrarily oriented in a cross-section of the fiber, it can be split into two orthogonal modes propagating with the same magnitude of wavenumber. These are designated as *degenerate modes*.

Application of (17) to a case of degenerate modes for a single-mode waveguide requires special caution. Assume a pair of degenerate modes with imaginary z components (this example is used by Ulrich and Simon [9])

$$\mathbf{E}_1 = -\frac{\mu' \mathbf{H}_2}{\sqrt{\mu_0 \epsilon_0}} = \{E_1^x, E_1^y, E_1^z\} = \left\{ J_0(r), 0, \frac{i}{k_1} \cos \phi J_0(r) \right\} \quad (18a)$$

and

$$\mathbf{E}_2 = \frac{\mu' \mathbf{H}_1}{\sqrt{\mu \epsilon_0}} = \{E_2^x, E_2^y, E_2^z\} = \left\{ 0, J_0(r), \frac{i}{k_1} \sin \phi J_0(r) \right\}, \quad (18b)$$

where ϕ is a polar angle in the cross sectional area A , $J_0(r) = dJ_0/dr$, k_1 is the wavenumber in the first (degenerate) mode, and the components are nondimensional. If (18) is inserted into (17) and the latter is applied without modification, one obtains

$$\begin{aligned} W_m &= \delta_{mn} \oint [(\hat{i}E_m^x + \hat{j}E_m^y) \times (\hat{i}H_n^x + \hat{j}H_n^y)] dA \\ &= \delta_{mn} \oint (E_m^x H_n^{y*} - E_m^y H_n^{x*}) dA. \end{aligned} \quad (19)$$

Since the goal of this analysis is to find the ratio a'_m/a_m , we are required to reduce the sum on $a'_m(z)$ to one term. We therefore multiply the \hat{i} component of (15) by H_n^{y*} and the \hat{j} component by H_n^{x*} . When $m \neq n$, Eq. (19) is zero as required. However, if $m = 1$ and $n = 2$, it is seen from (18a) that H_n^{y*} is zero. Hence *all* terms in the \hat{i} component will be zero. We will therefore not be able to use this sum to find a relation for a'_m in terms of a_m . On the other hand, H_2^z is not zero, thus the \hat{j} component can be used. To avoid this difficulty, we use a second orthogonality,

$$\begin{aligned} W_m \delta_{mn} &= \oint (H_m^t * \times E_n^t)^z dA \\ &= \oint (H_m^x * E_n^y - H_m^y E_n^{x*}) dA, \end{aligned} \quad (20)$$

Again, when $m = 1$ and $n = 2$, one multiplies the \hat{i} component of (15) by H_1^y . Since this is not zero, the \hat{i} component will yield a relation between a'_m and a_m . In contrast, multiplication of the \hat{i} component of (15) by H_1^x causes all terms to vanish. These thoughts lead to the following summary: to apply orthogonality of modes to (15), we multiply the \hat{i} component by H_m^y and the \hat{j} component by H_n^x , and then integrate over the cross-sectional area of the fiber. The result is

$$\begin{aligned} \sum_n e^{ik_n z} \left\{ 2ik_m a'_n(z) \oint H_m^y E_n^x dA + a_n \epsilon_0^{-1} k^2 \oint H_m^y (\mathbf{U} \mathbf{E}_n)^x dA \right. \\ \left. + a_n \epsilon_0^{-1} \oint H_m^y \left[\frac{\partial^2}{\partial x^2} (\mathbf{U} \mathbf{E}_n)^x + \frac{\partial^2}{\partial x \partial y} (\mathbf{U} \mathbf{E}_n)^y \right] dA \right\} \\ + \sum_n a_n \epsilon_0^{-1} \left[\oint H_m^y \frac{\partial^2}{\partial x \partial z} e^{ik_n z} (\mathbf{U} \mathbf{E}_n)^z dA \right] = 0 \end{aligned} \quad (21a)$$

and

$$\begin{aligned} \sum_m e^{ik_m z} \left\{ 2ik_m a'_m(z) \oint E_m^y H_n^x dA + a_m \epsilon_0^{-1} k^2 \oint (\mathbf{U} \mathbf{E}_m)^y H_n^x dA \right. \\ \left. + a_m \epsilon_0^{-1} \oint \left[\frac{\partial^2}{\partial y \partial x} (\mathbf{U} \mathbf{E}_m)^x + \frac{\partial^2}{\partial y^2} (\mathbf{U} \mathbf{E}_m)^y \right] H_n^x dA \right\} \\ + \sum_m a_m \epsilon_0^{-1} \left[\oint \frac{\partial^2}{\partial y \partial z} e^{ik_m z} (\mathbf{U} \mathbf{E}_m)^z H_n^x dA \right] = 0. \end{aligned} \quad (21b)$$

These equations can be recast to bring out the concept of mode coupling.

Let $m = 1$ in Eqs. (21a) and (21b). Then, adding the two together, one obtains

$$e^{ik_1 z} 2ik_1 a'_1(z) I_{11}^{(0)} = - \sum_n e^{ik_n z} a_n [\epsilon_0^{-1} k^2 I_{1n}^{(1)} + \epsilon_0^{-1} I_{1n}^{(2)}] \quad (22a)$$

$$I_{1n}^{(1)} = \oint H_1^y (\mathbf{U} \mathbf{E}_n)^x dA + \oint (\mathbf{U} \mathbf{E}_1)^y H_n^x dA, \quad (22b)$$

and

$$I_{1n}^{(2)} = \oint H_1^y \left[\frac{\partial^2}{\partial x^2} (\mathbf{U} \mathbf{E}_n)^x + \frac{\partial^2}{\partial x \partial y} (\mathbf{U} \mathbf{E}_n)^y \right] dA + \oint \left[\frac{\partial^2}{\partial x \partial y} (\mathbf{U} \mathbf{E}_1)^x + \frac{\partial^2}{\partial y^2} (\mathbf{U} \mathbf{E}_1)^y \right] H_n^x dA. \quad (22c)$$

Define

$$A_m(z) = e^{ik_m z} a_m(z) \text{ and } A'_m(z) = a'_m(z) e^{ik_m z} + ik_m A_m(z). \quad (23)$$

Since

$$a_1'(z)e^{ik_1 z} = -\frac{\sum_n e^{ik_n z} a_n [\epsilon_0^{-1} k^2 I_{1n}^{(1)} + \epsilon_0^{-1} I_{1n}^{(2)}]}{2ik_1 I_{11}^{(0)}} \quad (24)$$

$$= i \sum_n \kappa_{1n} A_n,$$

it is seen that

$$A_1'(z) = ik_1 A_1(z) + i \sum_n \kappa_{1n} A_n \quad (25)$$

and

$$\kappa_{1n} = \frac{\epsilon_0^{-1} k^2 I_{1n}^{(1)} + \epsilon_0^{-1} I_{1n}^{(2)}}{2k_1 I_{11}^{(0)}}. \quad (26)$$

Similar formulas are obtained for $m = 2$. The quantities κ_{mn} are the mode coupling coefficients. They describe how the dielectric polarization caused by the dyadic \mathbf{U} makes the expansion coefficient a_m of one mode depend on the coefficients of all other modes. A particular case of mode coupling of primary interest here is the photoelastic effect, in which \mathbf{U} describes the interaction of light and mechanical stress. This is described next for the case of torsional stress.

Dielectric Polarization by Torsional Stress

The dyadic operation $\mathbf{U}\mathbf{E}$ yields a vector with three components:

$$(\mathbf{U}\mathbf{E})^x = U_{xx} E^x + U_{xy} E^y + U_{xz} E^z, \quad (27a)$$

$$(\mathbf{U}\mathbf{E})^y = U_{yx} E^x + U_{yy} E^y + U_{yz} E^z, \quad (27b)$$

and

$$(\mathbf{U}\mathbf{E})^z = U_{zx} E^x + U_{zy} E^y + U_{zz} E^z. \quad (27c)$$

When the fiber is strained in pure torsion (Fig. 5), the displacements for a twist τ (angle per unit length) are

$$u_x = -\tau zy \text{ and } u_y = \tau zx. \quad (28)$$

The strains are then

$$S_{xz} = S_{zx} = \left(\frac{\partial u_x}{\partial z} + \frac{\partial u_z}{\partial x} \right) = -\tau y \quad (29a)$$

and

$$S_{yz} = S_{zy} = \left(\frac{\partial u_y}{\partial z} + \frac{\partial u_z}{\partial y} \right) = \tau x. \quad (29b)$$

Now the components of the dyadic \mathbf{U} are proportional to the strain components,

$$U_{ij} = gS_{ij}. \quad (30)$$

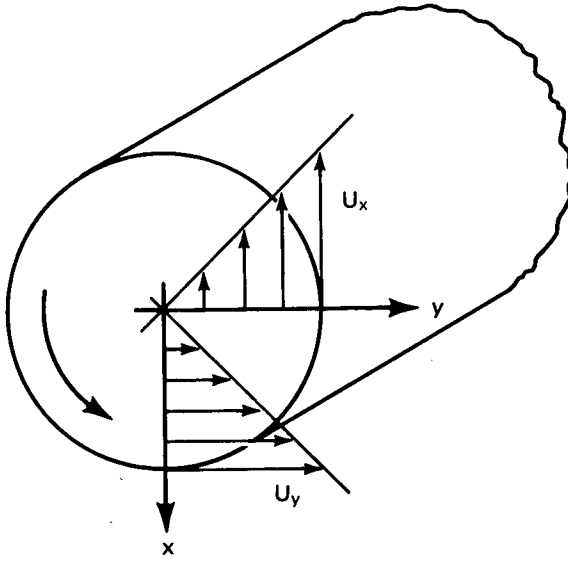


Fig. 5 – Torsional displacements

The dielectric polarization thus reduces to the following components:

$$(\mathbf{U}\mathbf{E})^x = -g\tau y E^z = -g\tau r \sin \phi E^z, \quad (31a)$$

$$(\mathbf{U}\mathbf{E})^y = g\tau x E^z = g\tau r \cos \phi E^z, \quad (31b)$$

and

$$(\mathbf{U}\mathbf{E})^z = -g\tau y E^x + g\tau x E^y = -g\tau r \sin \phi E^x + g\tau r \cos \phi E^y. \quad (31c)$$

We shall use these components to calculate mode coupling coefficients for the case of pure torsion.

Mode Coupling Coefficients for Pure Torsion

The calculation for the case $m = 1, n = 2$ will proceed in steps. From Eq. (21a),

$$\begin{aligned} \oint H_1^y (\mathbf{U}\mathbf{E}_2)^x dA &= \oint \frac{\sqrt{\mu\epsilon_0}}{\mu'} J_0(r) (-g\tau) r \sin^2 \phi \frac{i}{k_1} \dot{J}_0(r) dA \\ &= -i \frac{\sqrt{\mu\epsilon_0}}{k_1 \mu'} g\tau \oint r \sin^2 \phi J_0(r) \dot{J}_0(r) dA \end{aligned} \quad (32a)$$

and

$$\begin{aligned} \oint H_1^y \frac{\partial^2}{\partial x \partial y} (\mathbf{U}\mathbf{E}_2)^y &= \oint \frac{\sqrt{\mu\epsilon_0}}{\mu'} J_0(r) \frac{\partial^2}{\partial x \partial y} g\tau \frac{i}{k_1} \frac{y}{r} \dot{J}_0(r) dA \\ &= i \frac{\sqrt{\mu\epsilon_0}}{\mu'} \frac{g\tau}{k_1} \oint \frac{J_0(r) \dot{J}_0(r)}{r} dA. \end{aligned} \quad (32b)$$

In Eq. (21b) we calculate

$$\begin{aligned} \oint (\mathbf{U}\mathbf{E}_1)^y H_2^x dA &= \oint g\tau r \cos \phi \frac{(-i)}{k_1} \cos \phi \dot{J}_0(r) \frac{\sqrt{\mu\epsilon_0}}{\mu'} J_0(r) dA \\ &= -i \frac{\sqrt{\mu\epsilon_0}}{k_1 \mu'} g\tau \oint r \cos^2 \phi \dot{J}_0(r) J_0(r) dA \end{aligned} \quad (32c)$$

and

$$\oint \frac{\partial^2}{\partial y \partial x} (\mathbf{U} \mathbf{E}_1)^x H_2^x dA = \oint \frac{\partial^2}{\partial y \partial x} \left[-g\tau y \frac{i}{k_1} \frac{x}{r} j_0(r) \frac{-\sqrt{\mu\epsilon_0}}{\mu'} J_0(r) \right] dA \quad (32d)$$

$$= g\tau \frac{i}{k_1} \frac{\sqrt{\mu\epsilon_0}}{\mu'} \oint \frac{J_0(r) j_0(r)}{r} dA.$$

We omit for the moment the calculation of the third terms in (21a) and (21b). Adding Eqs. (32a) and (32c), one obtains

$$I_{12}^{(1)} = \frac{-i\sqrt{\mu\epsilon_0}}{k_1 \mu'} g\tau 2\pi \int_0^R r^2 J_0(r) j_0(r) dr. \quad (33a)$$

Integration by parts leads to

$$\int_0^R [J_0(r) j_0(r)] r^2 dr = \frac{J_0^2(r)}{2} r^2 \Big|_0^R - \int_0^R \frac{J_0^2(r)}{2} 2r dr$$

$$= - \int_0^R J_0^2(r) r dr.$$

Hence,

$$I_{12}^{(1)} = \frac{i\sqrt{\mu\epsilon_0}}{k_1 \mu'} g\tau 2\pi \int_0^R J_0^2(r) r dr. \quad (33b)$$

Next we calculate

$$\oint H_1^y E_1^x dA = 2\pi \int_0^R \frac{\sqrt{\mu\epsilon_0}}{\mu'} J_0^2(r) r dr, \quad (34a)$$

$$\oint E_1^y H_1^x dA = 0, \quad (34b)$$

$$\oint H_2^y E_2^x dA = 0, \quad (34c)$$

and

$$\int E_2^y H_2^x dA = -2\pi \int_0^R \frac{\sqrt{\mu\epsilon_0}}{\mu'} J_0^2(r) r dr. \quad (34d)$$

We combine (34a) and (34b) and combine (34c) and (34d), and get

$$I_{11}^{(0)} = 2\pi \int_0^R \frac{\sqrt{\mu\epsilon_0}}{\mu'} J_0^2(r) r dr \quad (34e)$$

and

$$I_{22}^{(0)} = -I_{11}^{(0)}. \quad (34f)$$

These quantities will now be used to find a'_m of a_m .

As an example, let $n = 2$. Then

$$\kappa_{12} = \frac{\epsilon_0^{-1} k^2 \frac{i\sqrt{\mu\epsilon_0}}{k_1 \mu'} g\tau 2\pi \int_0^R J_0^2(r) r dr + i\epsilon_0^{-1} \frac{\sqrt{\mu\epsilon_0}}{\mu'} \frac{g\tau}{k_1} 2\pi \int_0^R J_0(r) j_0(r) dr}{4\pi k_1 \frac{\sqrt{\mu\epsilon_0}}{\mu'} \int_0^R J_0^2(r) r dr}.$$

Now when r is very small, $J_0(r) \rightarrow 0$, hence we neglect $I_{12}^{(2)}$. Thus,

$$\kappa_{12} = \frac{i\epsilon_0^{-1} k^2}{2k_1^2} g\tau.$$

If

$$g = p_{44} n_0^4 \epsilon_0 \text{ and } n_0^{-1} = k/k_1,$$

then

$$\kappa_{12} = \frac{i}{2} \epsilon_0^{-1} \frac{\tau}{n_0^2} p_{44} n_0^4 \epsilon_0 = \frac{i\tau}{2} p_{44} n_0^2.$$

This result is identical (except for sign) with that of Ulrich and Simon [9].

Since m and n are dummy indices when they appear in Eqs. (21a) and (21b), it is seen from (34f) that

$$\kappa_{12} = -\kappa_{21}.$$

We return briefly to the third terms in (21a) and (21b). They both cancel for $m = 1, n = 2$:

$$\begin{aligned} \oint H_1^y \frac{\partial^2}{\partial x \partial z} e^{ik_2 z} (\mathbf{U} \mathbf{E}_2)^z dA &= \oint \frac{\sqrt{\mu\epsilon_0}}{\mu'} J_0(r) ik_2 \frac{\partial}{\partial x} [-g\tau y \cdot 0 + g\tau x J_0(r)] dA e^{ik_2 z} \\ &= -g\tau ik_2 \frac{\sqrt{\mu\epsilon_0}}{\mu'} \oint J_0^2(r) dA e^{ik_2 z} \end{aligned}$$

and

$$\oint ik_1 e^{ik_1 z} \frac{\partial^2}{\partial y \partial z} [-g\tau y J_0(r) + g\tau x \cdot 0] \frac{\sqrt{\mu\epsilon_0}}{\mu'} (-) J_0(r) dA = ik_1 e^{ik_1 z} g\tau \frac{\sqrt{\mu\epsilon_0}}{\mu'} \oint J_0^2(r) dA.$$

Since $k_1 = k_2$ (modes are degenerate), the z -components cancel.

We next consider the mode coupling for the case of $m = 1, n = 1$:

$$\oint H_1^y (\mathbf{U} \mathbf{E}_1)^x dA = \oint J_0(r) \frac{\sqrt{\mu\epsilon_0}}{\mu'} \left[-g\tau r \sin \phi \frac{i}{k_1} \cos \phi J_0(r) \right].$$

Now $\int_0^{2\pi} \sin \phi \cos \phi d\phi = 0$, hence this integral is zero and

$$\oint (\mathbf{U} \mathbf{E}_1)^y H_1^x dA = \oint g\tau r \cos^2 \phi \frac{i}{k_1} J_0(r) \cdot 0 = 0,$$

$$\oint H_1^x \frac{\partial^2}{\partial x \partial y} (\mathbf{U} \mathbf{E}_1)^y dA = \oint J_0(r) \frac{\sqrt{\mu\epsilon_0}}{\mu'} \frac{\partial^2}{\partial x \partial y} \left[g\tau \frac{x^2}{r} \frac{i}{k_1} J_0(r) \right] dA = 0,$$

$$\oint \frac{\partial^2}{\partial y \partial x} (\mathbf{U} \mathbf{E}_1)^x H_1^y dA = \oint \frac{\partial^2}{\partial y \partial x} \left[-g\tau y \frac{x}{r} \frac{i}{k_1} J_0(r) \right] dA \cdot 0 = 0,$$

$$\oint H_1^x \frac{\partial}{\partial x \partial z} e^{ik_1 z} (\mathbf{U} \mathbf{E}_1)^z dA = \oint \frac{\sqrt{\mu\epsilon_0}}{\mu'} J_0(r) ik_1 e^{ik_1 z} \frac{\partial}{\partial x} [-g\tau y J_0(r) + g\tau x \cdot 0] dA = 0$$

and

$$\oint \frac{\partial^2}{\partial y \partial z} e^{ik_1 z} (\mathbf{U} \mathbf{E}_1)^z H_1^y = 0.$$

From this it is seen that $\kappa_{11} = 0$. Also, since m and n are dummy indices when used together, it is seen that $\kappa_{22} = 0$.

Discussion: When $m = n$, κ_{mn} expresses the condition that the energy density $\mathbf{E} \cdot \mathbf{D}$ is no longer a sum of diagonal terms, because each component of a single mode is coupled to the other two components through \mathbf{U} . The mode is said to be *detuned*. When $m \neq n$ the disturbance couples a component of one mode to the components of the second mode. Such coupling is forbidden in the undisturbed material, but it is the origin of experimentally observed twist effects.

Evolution of Electric Vector Polarization in the Case of Pure Torsion of a Fiber

The set of coupled equations in A_m is now applied to two degenerate modes:

$$\frac{dA_1}{dz} = i\kappa_{11} A_1 + i\kappa_{12} A_2$$

and

$$\frac{dA_2}{dz} = i\kappa_{21} A_1 + i\kappa_{22} A_2.$$

Since A_1 and A_2 are complex numbers, a convenient transformation of this set can be made in terms of ψ and ϕ , representing their normalized amplitude difference and their normalized phase difference, respectively. The mean amplitude C and mean phase Φ do not contribute to mode coupling and so are not considered. By further introducing the spatial beat frequency $2\delta = \kappa_{11} - \kappa_{12}$, and assuming a lossless fiber, $\kappa_{12} = \kappa_{21}^* = |\kappa_{12}|e^{i\gamma}$, Ulrich [10] shows that the angular velocity Ω and direction of the axis R of rotation are given by

$$\Omega = 2(\delta^2 + \kappa^2)^{1/2} = |(\kappa_{11} - \kappa_{22})^2 + 4\kappa_{12}\kappa_{21}^*|^{1/2},$$

$$2\psi_R = \arctan \frac{\delta}{\kappa} = \arctan \left| \frac{\kappa_{11} - \kappa_{22}}{\sqrt{4\kappa_{12}\kappa_{21}^*}} \right|,$$

and

$$2\phi_R = \arg \kappa_{12} = \gamma.$$

Thus an evaluation of the mode coupling coefficients κ_{mn} gives directly the location of the axis of rotation and the rotation per unit of length.

These results may now be used to find the magnitude and direction of the axis of rotation in the case of pure torsion:

$$|\Omega| = |4\kappa_{12}\kappa_{21}^*|^{1/2} = 2|\kappa_{12}| = \tau|p_{44}|n_0^2 \quad (\text{units: rad/m}),$$

$$2\chi = 2\psi_R = \arctan(0) = 0,$$

and

$$2\psi = 2\phi_R = \arg \kappa_{12} = -90^\circ.$$

Since $|\phi_R| = 45^\circ$, it is seen from the properties of the Poincaré sphere S that the two modes are in *time-phase quadrature*, hence the polarization is circularly birefringent. Also, since $\psi_R = 0$, it is seen

that the amplitudes of the two modes are always equal, hence the trajectory of the state of polarization is the equator of the sphere S . Therefore, the axis of rotation is LR and the rotation vector is α .

Choose now a fiber of fused silica. Then the angular velocity of the trajectory is

$$|\Omega| = |-0.075|(1.46)^2\tau = 0.16\tau.$$

Actual measurements show [9]

$$\frac{d}{\tau} = +0.13 \pm 0.01.$$

From this discussion of Ulrich and Simon's work it is seen that these results apply only to pure twist-induced optical activity. Next we include birefringence.

The optical activity rotation about LR is described by $\alpha - 2\tau$, while the birefringent rotation about HV is described by β . When the two rotations are combined, the state of polarization traces out a cycloidal trajectory, that is, the circular trajectory traced out by the tip of the $C(z)$ unit vector in the local coordinate system is added to the trajectory of the unit vector as it moves around a latitude circle located at angle of elevation 2ψ , where

$$2\psi = \arctan\left(\frac{\alpha - 2\tau}{\beta}\right).$$

To illustrate the use of these results, Ref. 9 solves the problem of the use of a fiber of length L , fixed at its ends and twisted at the center through such an angle θ that the fast and slow modes are interchanged in their powers at the output. To achieve this, one sets

$$2\psi = \pm\pi/4$$

and

$$\Omega L = \pi.$$

Thus,

$$\frac{\alpha - 2\tau}{\beta} = 1,$$

$$\Omega = [\beta^2 + (\alpha - 2\tau)^2]^{1/2} = \sqrt{2}\beta,$$

and

$$L = \frac{\pi}{\sqrt{2}\beta}.$$

The required θ is then

$$\theta = \tau L = \frac{\tau \pi}{\sqrt{2}\beta} = \frac{\tau \pi}{\sqrt{2}(\alpha - 2\tau)}$$

$$= \frac{\pi}{\sqrt{2}|g - 2|},$$

where

$$g = \frac{\alpha}{\tau}.$$

For a fused silica step-indexed fiber $g = 0.13$, so,

$$\theta = \frac{\pi}{\sqrt{2}} \frac{1}{1.87} = 68^\circ.$$

Thus, if a length L is double-twisted at its center $\pm 68^\circ$ there is an interchange of slow and fast modes.

Periodic Dielectric Polarization

When the dielectric polarization is periodic in space and time it can be represented in real form by

$$\mathbf{P} = \mathbf{U}\mathbf{E} = \mathbf{U}(\mathbf{r}, t)\mathbf{E}\cos\Omega\left[t - \frac{z}{V}\right] \quad (35a)$$

and

$$V = \frac{\Omega}{K}, \quad (35b)$$

in which K is the spatial wavenumber of the elements of \mathbf{U} and Ω is the associated angular frequency. With this form of \mathbf{P} the propagation of \mathbf{E} is found from Eq. (7) to be

$$\begin{aligned} \nabla^2\mathbf{E} - \mu'\epsilon_0\frac{\partial^2\mathbf{E}}{\partial t^2} &= \epsilon_0^{-1}(\nabla\epsilon_0 \cdot \mathbf{E}) + \epsilon_0^{-1}\mu'\frac{\partial^2}{\partial t^2}\left[\mathbf{U}(\mathbf{r}, t)\mathbf{E}\cos\Omega\left[t - \frac{z}{V}\right]\right] \\ &+ \epsilon_0^{-1}\nabla \cdot \left[\mathbf{U}(\mathbf{r}, t)\mathbf{E}\cos\Omega\left[t - \frac{z}{V}\right]\right]. \end{aligned} \quad (36)$$

In the case of a homogeneous glass optical fiber under mechanical stress an approximate model for \mathbf{E} can be obtained if one assumes that

$$\nabla\epsilon_0 \rightarrow 0, \quad (37a)$$

$$\mathbf{E} = \mathbf{E}(\mathbf{r})e^{i\omega t}, \quad \omega \gg \Omega, \quad (37b)$$

$$\mu' \approx \mu_0, \quad (37c)$$

and

$$\mathbf{U}(\mathbf{r}, t) \rightarrow \mathbf{U}(\mathbf{r}). \quad (37d)$$

Then

$$\begin{aligned} \nabla^2\mathbf{E}(\mathbf{r}) + k^2\mathbf{E}(\mathbf{r}) &= -\epsilon_0^{-1}\mu'[\mathbf{U}(\mathbf{r})\mathbf{E}]\Omega^2\cos\Omega\left[t - \frac{z}{V}\right] \\ &+ \epsilon_0^{-1}\nabla \cdot \left[\mathbf{U}(\mathbf{r})\mathbf{E}\cos\Omega\left[t - \frac{z}{V}\right]\right]. \end{aligned} \quad (38)$$

From this it is seen that all electric field polarization effects discussed earlier in this report will become periodic with period $T = 2\pi/\Omega$.

ANALYSIS BY PHOTOELASTICITY OF ELECTRIC FIELD POLARIZATION OF SINGLE MODE FIBERS UNDER MECHANICAL STRESS

In previous sections of this report the optical fiber was assumed to be carrying two degenerate modes although its physical construction was "single mode." Also, the dielectric polarization $\mathbf{U}\mathbf{E}$ was assumed to be caused by applied elastic strains. We next consider the case of single-mode fibers carrying only one mode and assume $\mathbf{U}\mathbf{E}$ to be caused by applied elastic stresses. The theory of the electric field polarization in this case is the classical one of photoelasticity. Our objective in the following sections is to make numerical estimates of the changes in index of refraction of optical fibers with applied mechanical stress. To have a substantial basis for assuring the validity of these estimates, it is necessary to review the fundamentals of the theory of photoelasticity.

Stress Analysis

Mechanical stress in an elastic body is represented by a matrix of forces acting on an elementary volume centered at a point. The matrix T in three-dimensions (x, y, z) has nine components T_{ij} ($i = x, y, z; j = x, y, z$). The first subscript indicates the x, y , or z component of the force through the point; the second subscript indicates the coordinate plane through the point on which the component acts. In two dimensions (say coordinates x, y) the matrix has four components of *plane stress*. In isotropic materials the off-diagonal components are equal, thus reducing the state of plane stress to only three distinct components, namely, two normal stresses, σ_x and σ_y , and one shear stress $\tau_{xy} (= \tau_{yx})$. Through the center of the stress volume, in the plane of plane stress, there is always one direction (the trace of a normal plane) in which the normal stress (p) is a maximum, and an associated orthogonal direction (or plane) in which a second normal stress (q) is a minimum (Fig. 6). These are the *principal directions* (or *planes*) of stress at the point. In these directions the shear stress vanishes. Rotation of these directions about the center causes the shear to grow until it reaches a maximum at a rotation of 45° . When the stress at a point is three dimensional, one can create a condition of plane stress by choosing *any* direction through the point and calculating the stresses on a plane perpendicular to this direction. On this plane one can then locate the orthogonal directions of the *secondary principal stresses* by formulas given in later sections.

The existence of primary principal stresses in two-dimensional stress and secondary principal stresses in three-dimensional stress determines the state of polarization of light propagating through the point in a stressed body. This is considered next.

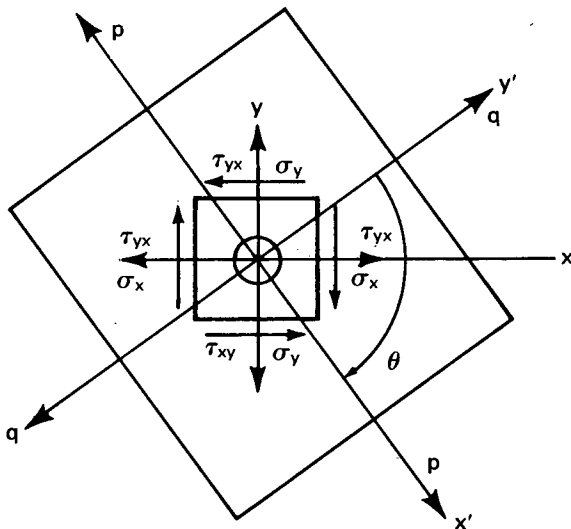


Fig. 6 — Principal axes of plane strain

Propagation of Polarized Light in Doubly Refracting Materials

Every elementary volume centered at a point of an elastic body under mechanical stress exhibits temporary double refraction to polarized light, provided certain conditions are fulfilled. Upon entering the volume in a given direction through its center, the light ray may encounter a state of local plane stress on a plane through the center transverse to the incident direction. These are the stresses that alter the state of polarization of the light. *No other stress components have any effect on polarization.* The light vector oscillating transverse to the direction of propagation sees only two orthogonal planes upon which it can vibrate, all other planes being effectively prohibited. These are the planes of primary or secondary principal stresses, whose traces are in the transverse plane. The light therefore splits into two components: one component travels with its light vector parallel to one principal plane, and the

second component travels with its light vector parallel to the orthogonal principal plane. The speed of travel of each component is determined by the value of the principal stress it encounters along its path. Since the principal stresses are generally different in sign and magnitude, one component travels on a fast axis (or plane) and the second component on a slow axis (or plane). If the incident light is of a single frequency, this difference in speed between the two beams displays itself as a difference in phase $(k_{\text{fast}} - k_{\text{slow}})z$ at each coordinate distance z of the path, k being the wavenumber of the propagating light. The relation of altered wavenumbers k_{fast} and k_{slow} to the mechanical stresses p and q forms the basis of the theory of photoelasticity. This is discussed next.

Repeated experiments have established the *stress-optic law* that $k_{\text{fast}} - k_{\text{slow}}$ is proportional to $p - q$; that is, the difference in wavenumber is directly proportional to the difference of principal stresses in the transverse plane. If the incident polarized light of single wavelength λ_0 propagates through a thickness d of a stressed elastic body, the two components exit with a phase difference of

$$\Delta\phi_d = k_0 C(p - q)d,$$

where $k_0 = 2\pi/\lambda_0$, C is the stress-optic constant of the material, and $p - q$ is the difference of primary or secondary principal stresses in the transverse plane. An estimation of this phase difference and the state of exit polarization of the two component beams requires careful consideration. This is now reviewed.

Polarization Effects in Stressed Elastic Bodies

Assume first that the incident light is plane polarized at an angle α with the x axis in an xy coordinate system, and assume that the coordinate axes are principal axes of stress. The plane xy is transverse to the incident ray (Fig. 7). The incident light vector is represented as a simple sinusoid,

$$\mathbf{s} = \mathbf{a} \cos \omega t.$$

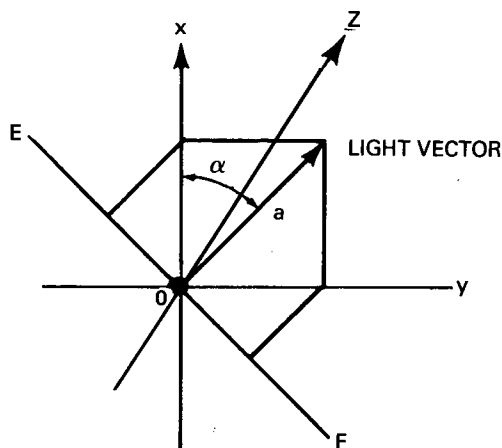


Fig. 7 — Linearly polarized light in a stressed body

It splits into two unique components (no other components effectively propagating) initially synchronized (that is, having the same temporal phase),

$$s_x = a \cos \alpha \cos \omega t \text{ and } s_y = a \sin \alpha \cos \omega t.$$

These components travel along the principal planes of (two-dimensional) stress at different speeds, V_x and V_y . After a propagation distance d they become unsynchronized,

$$s_x = a^* \cos(\omega t + \Delta\phi_1),$$

$$s_y = b^* \cos(\omega t + \Delta\phi_2),$$

$$a^* = a \cos \alpha,$$

$$b^* = a \sin \alpha,$$

$$\Delta\phi_1 = \frac{\omega}{V_x} z,$$

$$\Delta\phi_2 = \frac{\omega}{V_y} z,$$

and

$$(\Delta\phi_1 - \Delta\phi_2)/2 = \Delta\phi_d = k_0 C(p - q)d.$$

In the theory of photoelasticity the angle $\Delta\phi_d$ is measured to find the stress difference $p - q$. This is done by causing s_x and s_y to interfere in a selected plane of a polariscope. Choosing plane EF perpendicular to the incident light vector, one finds the amplitude of the resultant vibration to be [11, p. 124]

$$B = a \sin 2\alpha \sin \Delta\phi_d.$$

If $p - q$ is zero, B is zero, meaning that the light transmitted through point O is extinguished when viewed on plane EF in a polariscope. A similar extinguishment occurs when

$$\Delta\phi_d = k_0 C(p - q)d = n\pi, \quad n = 1, 2, \dots$$

If the stress difference $p - q$ is a function of time,

$$p - q = p(t) - q(t),$$

then

$$B = (a \sin 2\alpha) \sin\{k_0 C[p(t) - q(t)]d\},$$

i.e., the light viewed in the polariscope on plane EF varies in amplitude with time.

If the propagation direction is z , then the light vector of Fig. 7 at any distance $z = \text{const.}$ is the vector sum of two unsynchronized components of different amplitude. Thus, in the plane $z = \text{const.}$ the total light vector rotates in time about the center in an elliptical motion. The stress difference $p - q$ can then be said to unsynchronize the initially synchronized components of the plane-polarized light along the principal axes. Since the unsynchronization varies with distance of propagation d , the major and minor axes of the elliptical motion of the light vector change continuously with increase in path. However, at any station $z = \text{const.}$ a polariscope will find a plane EF along which the transmission will be extinguished whenever $p - q$ reaches a level such that $\Delta\phi_d = n\pi$, $n = 1, 2, \dots$

Next we consider the case where the incident light ray at $z = 0$ has two equal-amplitude orthogonal components which are temporally unsynchronized by 90° :

$$s_x = a \cos \omega t$$

and

$$s_y = a \sin \omega t.$$

The light vector rotates in a circle about the center point of incidence in the plane $z = \text{const.}$ Assume that it rotates counterclockwise. Upon propagating a distance d through a stressed elastic body in which

$p - q$ in the transverse plane is finite, the two components of the light vector are further unsynchronized by the temporal phase $\Delta\phi_d$ defined above. Assume a reference axis y' along which the incremental phase vanishes. Then

$$s'_x = a \cos(\omega t + \Delta\phi_d) = a \sin(\omega t + \pi/2 + \Delta\phi_d)$$

and

$$s'_y = a \sin \omega t.$$

It can be shown [12, p. 94] that the motion of the resultant light vector at a local station where $z = \text{const}$ can be resolved into two oppositely rotating circular motions:

$$s_x^{(1)} = A \cos(\omega t + \gamma), \quad s_y^{(1)} = A \sin(\omega t + \gamma)$$

and

$$s_x^{(2)} = -B \cos(\omega t + \delta), \quad s_y^{(2)} = B \sin(\omega t + \delta),$$

where

$$A^2 = \frac{a^2}{2} \left[1 + \sin\left(\frac{\pi}{2} + \phi_d\right) \right],$$

$$\tan \gamma = - \frac{\cos\left(\frac{\pi}{2} + \phi_d\right)}{1 + \sin\left(\frac{\pi}{2} + \phi_d\right)},$$

$$B^2 = \frac{a^2}{2} \left[1 - \sin\left(\frac{\pi}{2} + \phi_d\right) \right],$$

and

$$\tan \delta = \frac{\cos\left(\frac{\pi}{2} + \phi_d\right)}{1 - \sin\left(\frac{\pi}{2} + \phi_d\right)}.$$

The combination of the two motions is equivalent to elliptical motion. Thus, the components of incident circularly polarized light are temporally unsynchronized more or less than 90° by mechanical stresses $p - q$, making the resultant elliptically polarized. As before, the angular location of the major and minor axes of the traced ellipse varies continuously with distance of propagation. Several possible conditions of polarization can be obtained:

- If the phase difference $\Delta\phi_d$ corresponds to an integral number of wavelengths ($2n\pi$, $n = 1, 2 \dots$), no change in the initial circularly polarized light results.
- If the phase difference corresponds to a half wavelength (plus any number of integral wavelengths), then $A = 0$, $B = a$, and the initial circularly by polarized light emerges with reversed direction of rotation.
- If the phase difference is arbitrary, A and B are finite and different, and the initial circularly polarized light emerges elliptically polarized.

Finally, we consider the case where the incident light has two orthogonal components with unequal amplitudes, temporally unsynchronized by 90° so that the resultant light vector traces an ellipse in a plane normal to the optic ray:

$$s_x = a \cos \omega t$$

and

$$s_y = b \sin \omega t.$$

If one sets [12, p. 94]

$$A^2 = \frac{1}{4} \left[a^2 + b^2 + 2ab \sin \left(\frac{\pi}{2} + \phi_d \right) \right],$$

$$B^2 = \frac{1}{4} \left[a^2 + b^2 - 2ab \sin \left(\frac{\pi}{2} + \phi_d \right) \right],$$

$$\tan \gamma = - \frac{a \cos \left(\frac{\pi}{2} + \phi_d \right)}{b + a \sin \left(\frac{\pi}{2} + \phi_d \right)},$$

and

$$\tan \delta = \frac{a \cos \left(\frac{\pi}{2} + \phi_d \right)}{b - a \sin \left(\frac{\pi}{2} + \phi_d \right)},$$

then it will be seen that

- If ϕ_d corresponds to an integral number of wavelengths, no change in polarization is to be expected.
- If ϕ_d corresponds to a half-wavelength, then the initial elliptical polarization emerges elliptically polarized with reversed rotation.
- If ϕ_d is arbitrary, the emerging light is also elliptically polarized with different sizes and directions of major and minor axes.

Summary

This completes our brief review of aspects of photoelasticity which are relevant to the study of the effects of mechanical stress on polarization of incident light. Photoelasticians use their tools to measure stresses p and q . The same tools in optical-fiber studies require the stresses to be known. We assume in subsequent sections that the stresses p and q can be estimated in specific examples. When the stresses are evaluated we can make numerical estimates of phase changes $\Delta\phi_d$. These are also estimates of changes in index of refraction Δn caused by stress birefringence. This is explained later in the report.

APPLICATIONS

Case 1. Applied Stress on the Fiber is Axisymmetric and Everywhere Uniform Along the Optical Path

Here the applied stress is a scalar pressure in the medium which exerts a force normal to the surface. The radial stress σ_r and the tangential stress σ_θ on a polar elementary volume are equal to each other and equal to the applied pressure [11, p. 55]. The principal stress difference $p - q$ is everywhere

zero. Hence there is no birefringent effect for an optic ray on the axis of the fiber. Thus, acoustic pressures in the sonar range of frequencies do not alter the state of polarization of light propagation in them. Similarly, hydrostatic pressures do not affect the phase of the light beam. It also does not matter what the time variation of the applied stress is, since no change in polarization of the incident light will occur as long as the stress is axisymmetric on the fiber.

Case 2. Applied Stress on the Fiber is Axisymmetric but Varies Along the Optic Path

Here again, as long as the applied stress is axisymmetric (that is, an applied scalar pressure), there is no birefringent effect for axial optic rays regardless of the nature of the variation of stress along the path of propagation.

Case 3. Tensile or Compressive Stresses are Applied to the Ends of the Fiber

In this case the fiber is uniformly stretched or compressed. All stresses inside the fiber on cross sections normal to the fiber axis are parallel to the propagating optic ray. Since there are no transverse components of stress for an axial optic ray, there is no birefringent effect. When, however, the incident optic ray is oblique to a selected plane of stresses, there is an effect. This is discussed next.

Case 4. Oblique Incidence of Optic Ray and Pure Bending

Figure 8 shows stress components on a three-dimensional elementary volume centered at $x(x, y, z)$ relative to the origin. The secondary principal stresses at x in direction i are defined (as noted previously) as the principal stresses resulting from stress components which lie in a plane transverse to i through x . These are designated $(p', q')_i$. As an example of secondary principal stresses choose the z direction. When σ_x and σ_y are present, one finds [13, p. 90]

$$(p', q')_z = \frac{\sigma_x + \sigma_y}{2} \pm \frac{1}{2} \sqrt{4\tau_{xy}^2 + (\sigma_x^2 - \sigma_y^2)}.$$

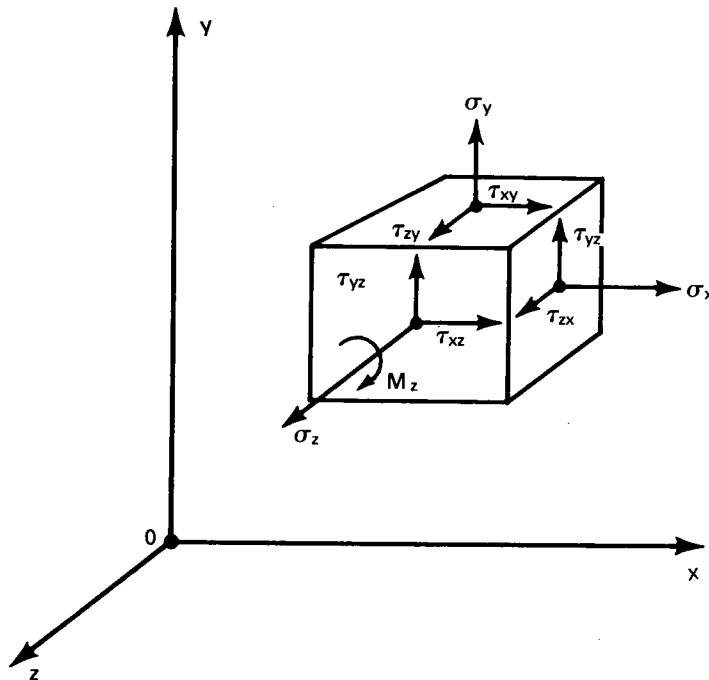


Fig. 8 — Stress components on a three-dimensional elementary volume

The orientation of p' and q' at center point x on the xy plane is along orthogonal axes rotated through an angle ϵ relative to the x axis,

$$(\tan 2\epsilon)_z = \frac{2\tau_{xy}}{\sigma_x - \sigma_y}.$$

An optic ray propagating in the coordinate direction z obeys the following rules: (1) Stress components subscripted with the letter z have no effect on the polarization. Thus, σ_z , τ_{yz} , and τ_{xz} have no effect. In particular, pure torsional moments M_z which produce τ_{yz} and τ_{xz} have no effect. (2) If the orientation of the secondary principal stresses rotates as the optic ray advances, the components of polarization also rotate.

When the optic ray is obliquely incident on the elementary volume, the birefringent retardation is calculated from transverse components. A simple example is a bar stretched by pure tension in the x direction (Fig. 9) and pierced by an optic ray in the z' direction parallel to the xz plane. Since stress components subscripted with the letter z' have no effect on polarization, the secondary principal stresses are

$$p' = \sigma_t \sin^2 \zeta$$

and

$$q' = 0.$$

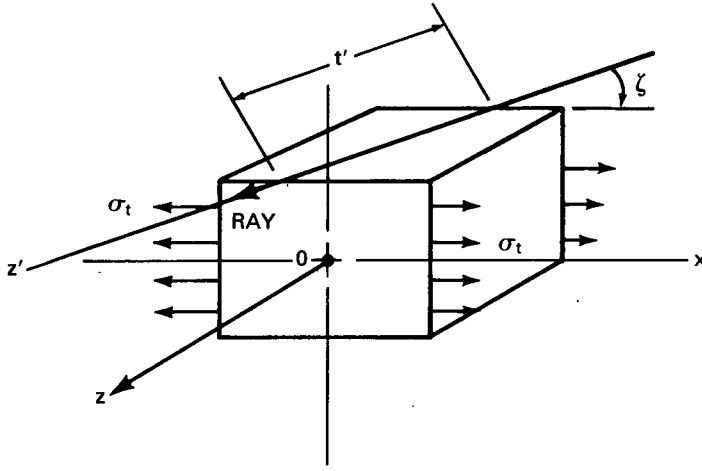


Fig. 9 — Oblique incidence of optic ray on an elementary volume

Defining *retardation* $R_d = m\lambda$ as the number m of wavelengths λ (generally not an integer) of difference in the phases of the birefringent components, one finds that the retardation along oblique path t' is then [14, p. 339],

$$R_d = m\lambda = Ct' \sigma_t \sin^2 \zeta = Ct \sigma_t \sin \zeta,$$

where

$$t = t' \sin \zeta.$$

This formula will be used in later numerical calculations. We next apply oblique incidence to pure bending of a bar lying along the x direction and bent by pure moments M_x at a cross section (Fig. 10). Let the optic ray be incident in the plane of the stresses σ at an angle ζ with the x axis. Assume that it enters an elementary volume at y and exits at y_0 . The secondary principal stresses at the center of the volume are

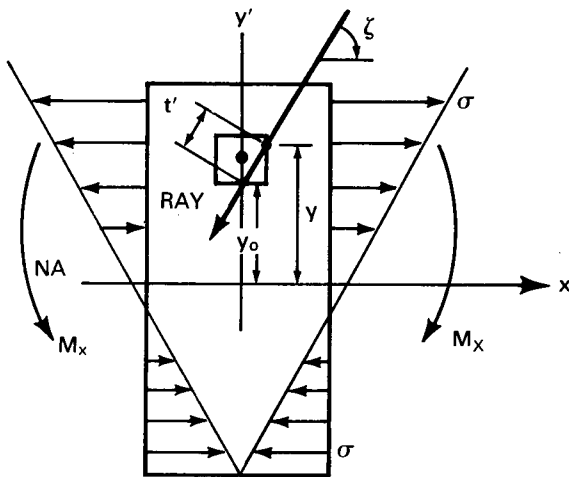


Fig. 10 — Oblique incidence in pure bending

$$p' = \frac{M_x y}{I_z} \sin^2 \zeta,$$

and

$$q' = 0,$$

in which I_z is the areal moment of inertia of the cross section about axis z . The retardation is [14, p. 348]

$$R_d = m\lambda = C \int_0^{t'} (p' - q') dt' = \frac{CM_x}{I_z} \sin \zeta \frac{(y^2 - y_0^2)}{2}.$$

Case 5. Fiber Subject to Both Bending and Shear

A fiber of circular cross section is subject to a bending moment M_x and a shear V_y at the ends of a segment whose thickness is in the x direction (Fig. 11). The normal stress at distance y from the neutral axis is

$$\sigma_x = \frac{M_x y}{I_z}.$$

The shear stresses τ for all points on line pp at a distance y_1 from the neutral axis all point toward the intersection S of tangent lines pS . Each τ has two components [14, p. 121],

$$\tau_{xy} = \tau \cos \beta = \frac{V(R^2 - y_1^2)}{3I_z}$$

and

$$\tau_{xz} = \tau \sin \beta = \frac{Vy_1 \sqrt{R^2 - y_1^2}}{3I_z},$$

where

$$\tau = \frac{VR \sqrt{R^2 - y_1^2}}{3I_z} = \sqrt{\tau_{xy}^2 + \tau_{xz}^2}.$$

where

$$\cos \psi = \cos \alpha_r \cos \alpha_p + \cos \beta_r \cos \beta_p$$

and

$$\cos \xi = \cos \alpha_r \cos \alpha_q + \cos \beta_r \cos \beta_q.$$

The retardation is then given by

$$m\lambda = C(p \sin^2 \psi - q \sin^2 \xi) t'.$$

Case 6. Fiber Wrapped on a Mandrel [15]

A circular fiber of diameter d is wrapped on a mandrel of radius r . A tangential force T is applied to the two open ends of the fiber to keep it tight. The stresses on a cross section at angle ϕ are analyzed with relation to the forces N and moments M shown in Fig. 12. These are

$$M = Tr(1 - \cos \phi),$$

$$N = T \cos \phi,$$

and

$$Q = T \sin \phi.$$

A cross section of the ring exhibits shear and bending (Fig. 13). The neutral axis of bending is orthogonal to the plane of the ring and passes through the axis of the fiber.

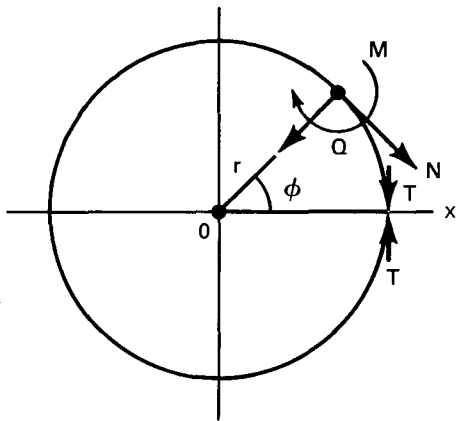


Fig. 12 — Forces on a fiber wrapped on a mandrel

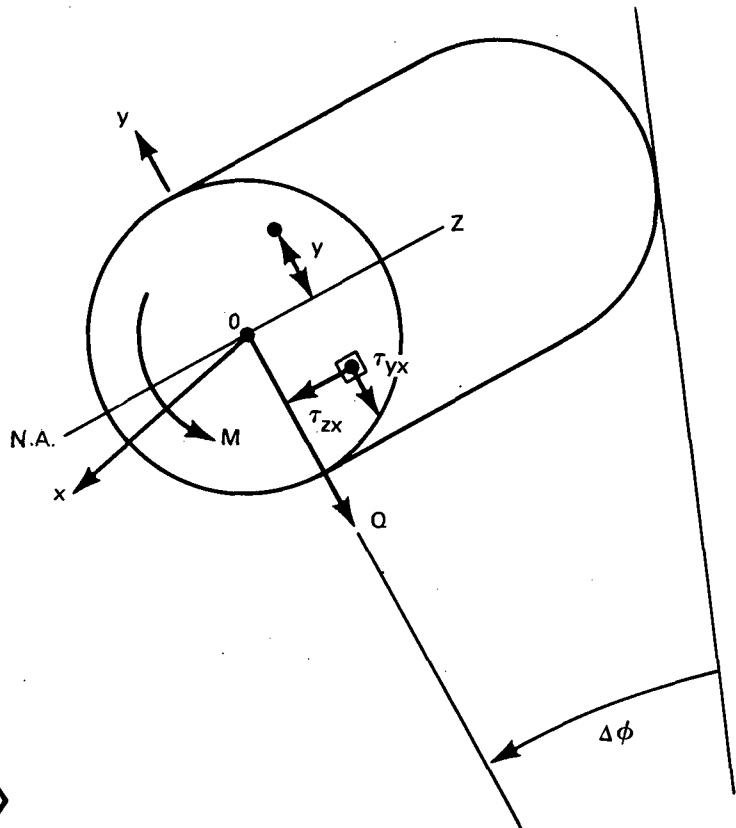


Fig. 13 — Shear Q and bending moment M on a cross section $\phi = \text{const}$

Let x represent the coordinate axis of the fiber, and y the perpendicular distance of any point from the neutral axis. Then the bending stress is

$$\sigma_x = \frac{My}{I_z},$$

where $I_z = \frac{\pi d^4}{64}$ and $M = 2Tr \sin^2 \frac{\phi}{2}$. Thus

$$\sigma_x = \frac{128 Tr y \sin^2 \frac{\phi}{2}}{\pi d^4}.$$

The shear stress consists of two components (see previous section),

$$\tau_{yx} = \frac{Q \left(\frac{d^2}{4} - y^2 \right)}{3I_z} = \frac{64}{3} \frac{1}{d^4} \left(\frac{d^2}{4} - y^2 \right) T \sin \phi$$

and

$$\tau_{zx} = \frac{Qy \left(\frac{d^2}{4} - y^2 \right)^{1/2}}{3I_z} = \frac{64}{3} y \frac{\left(\frac{d^2}{4} - y^2 \right)^{1/2}}{d^4} T \sin \phi,$$

and

$$\tau = \sqrt{\tau_{yx}^2 + \tau_{zx}^2} = \frac{32}{3} \frac{1}{d^3} \left(\frac{d^2}{4} - y^2 \right)^{1/2} T \sin \phi.$$

The principal stresses at point (y, z) lie in a plane normal to the yz plane:

$$p = \frac{\sigma_x}{2} + \left[\left(\frac{\sigma_x}{2} \right)^2 + \tau^2 \right]^{1/2}.$$

and

$$q = \frac{\sigma_x}{2} - \left[\left(\frac{\sigma_x}{2} \right)^2 + \tau^2 \right]^{1/2}.$$

They are on two orthogonal axes rotated about the z axis through an angle α given by

$$\tan 2\alpha = -\frac{2\tau}{\sigma_x}.$$

In terms of component shears we can write component principal stresses defined by

$$(p - q)_{y,x} = 2 \left\{ \left[\frac{64yTr \sin^2 \frac{\phi}{2}}{\pi d^4} \right]^2 + \left[\frac{32}{3} \frac{T \sin \phi \left(\frac{d^2}{4} - y^2 \right)}{d^4} \right]^2 \right\}^{1/2}$$

and

$$(p - q)_{z,x} = 2 \left\{ \left[\frac{64yTr \sin^2 \frac{\phi}{2}}{\pi d^4} \right]^2 + \left[\frac{32}{3} y \frac{T \sin \phi \left(\frac{d^2}{4} - y^2 \right)^{1/2}}{d^4} \right]^2 \right\}^{1/2}$$

The effect of these stress components on polarization depends on the angle of incidence of the optic ray. If the ray is along x exactly normal to the cross section the effect vanishes, since the subscripts of the stress components contain the letter x . Numerical calculations for optic rays obliquely incident on a cross section are given in a later section.

Case 7. Fiber Subject to Random Stresses

Let the stress fluctuations (defined as $\delta s = \delta(p - q)$) be randomly distributed along path length x . Assume that these stresses can be represented by a single scalar function of x . Then the mean-square phase after length L is reached is

$$\begin{aligned}\langle \delta\phi_L^2 \rangle &= \left\langle \left[\int_0^L k_0 C(x) \delta s(x) dx \right]^2 \right\rangle \\ &= k_0^2 C^2 \left\langle \left[\int_0^L \delta s(x) dx \right]^2 \right\rangle\end{aligned}$$

if $C(x) = C = \text{constant}$. In forming the square on the right-hand side, we must allow cross products at various values of x, x' , etc. To evaluate this integral we use Taylor's method [16]. By definition of the normalized autocorrelation function ρ ,

$$\int_0^x \langle \delta s(x) \delta s(x') \rangle dx' = \langle \delta s^2 \rangle \int_0^x \rho(x - x') dx'.$$

Since we always take the correlation ρ to be an even function, we can write the right hand side as

$$\langle \delta s^2 \rangle \int_0^x \rho(\xi) d\xi.$$

Now,

$$\int_0^x \langle \delta s(x) \delta s(x') \rangle dx' = \langle \delta s(x) \int_0^x \delta s(x') dx' \rangle = \langle \delta s(x) X \rangle,$$

where

$$X \equiv \int_0^x \delta s(x') dx'.$$

But

$$\langle \delta s(x) X \rangle = \frac{1}{2} \frac{d}{dx} \langle X^2 \rangle.$$

Thus, over a length L ,

$$\langle X^2 \rangle = 2 \langle \delta s^2 \rangle \int_0^L \int_0^x \rho(\xi) d\xi dx,$$

hence,

$$\langle \delta\phi_L^2 \rangle = k_0^2 C^2 \cdot 2 \langle \delta s^2 \rangle \int_0^L \int_0^x \rho(\xi) d\xi dx.$$

Two important cases can be distinguished:

(a) Suppose path length L is short enough so that $\rho(\xi)$ is essentially unity over the range of integration. This is the coherent case. Then

$$\sqrt{\langle \delta\phi_L^2 \rangle} = k_0 CL \sqrt{2 \langle \delta s^2 \rangle},$$

that is, the rms value of the phase is proportional to the length of the fiber.

(b) Assume L is so long that the stress at the end of the fiber is uncorrelated with the stress at the beginning of the fiber. This is the incoherent case. Then

$$\sqrt{\langle \delta\phi_L^2 \rangle} = k_0 C \sqrt{2 \langle \delta s^2 \rangle LL_c},$$

where

$$L_c = \int_0^\infty \rho(\xi) d\xi, \quad L_c \ll L.$$

In this case the rms phase is proportional to the square root of the length of the fiber. The symbol L_c represents the integral scale (or correlation length) of the random field.

In both cases we need the variance $\langle \delta s^2 \rangle$. This can be obtained from the spectral density δS_s of the stress distribution. By Rayleigh's theorem,

$$\int_{-\infty}^{\infty} |\delta s(x)|^2 dx = L \langle \delta s^2 \rangle = 2\pi \int_{-\infty}^{\infty} |\delta S_s(\alpha)|^2 d\alpha,$$

or

$$\langle \delta s^2 \rangle = \frac{2\pi}{L} \int_{-\infty}^{\infty} |\delta S_s(\alpha)|^2 d\alpha.$$

The spectral density must be determined by measurement.

Case 8. Fiber Squeezed by Diametral Forces: Circular Disk Model [11, p. 82]

A unit thickness of fiber is modeled as a circular disk (Fig. 14). Let two equal and opposite forces P (units: N/m) act along a diameter. The stress distribution is radial,

$$\sigma_r = -\frac{2P}{\pi} \frac{\cos \theta}{r}, \quad \sigma_\theta = 0, \quad \tau_{r\theta} = 0.$$

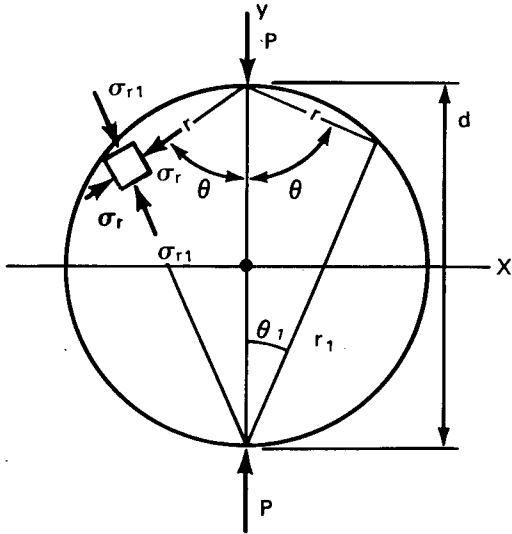


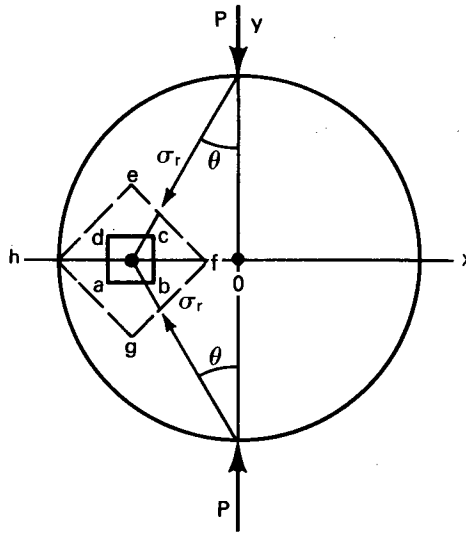
Fig. 14 — Fiber squeezed by diametral forces

Since $\frac{\cos \theta_1}{r_1} = \frac{\cos \theta_2}{r_2} = \frac{1}{D}$ and since $\tau_{r\theta} = 0$ the principal stresses on the circumference are

$$\sigma_{\min} = \sigma_{\max} = \sigma_r = -\frac{2P}{\pi D}.$$

For equilibrium one must superimpose tensions $2P/\pi D$ on each of these radial stresses. Suppose next the stresses on a horizontal diametral section are considered (Fig. 15). The normal stress on plane ac is contributed by two components of the σ_r 's,

Fig. 15 — Stresses on horizontal diameter



$$\sigma_y = -2 \left(\frac{2P}{\pi} \frac{\cos \theta}{r} \cdot \cos^2 \theta \right) + \frac{2P}{\pi D}$$

or

$$\sigma_y = \frac{2P}{\pi d} \left[1 - \frac{4D^2}{(D^2 + 4x^2)^2} \right]$$

On planes *bc*, *dc*, *ab*, and *ad* the shear stresses are all zero. The stress in the *x* direction is

$$\sigma_x = -\frac{4P}{\pi} \frac{\cos \theta}{r} \cdot \sin^2 \theta + \frac{2P}{\pi D}$$

Thus σ_x and σ_y are principal stresses, and their difference along a horizontal diameter is

$$\begin{aligned} p - q &= -\frac{4P \cos \theta}{\pi r} \sin^2 \theta + \frac{2P}{\pi D} + \frac{4P \cos \theta}{\pi r} \cos^2 \theta - \frac{2P}{\pi D} \\ &= \frac{4P \cos \theta}{\pi r} (\cos^2 \theta - \sin^2 \theta) = \frac{4P}{\pi r} \cos \theta (1 - 2\sin^2 \theta). \end{aligned}$$

At the center, $x = 0 = y$,

$$p - q = \frac{8P}{\pi D}$$

At the boundary, $x = \frac{D}{2}$, $y = 0$,

$$p - q = 0.$$

Numerical calculations of this case are given in a later section.

Case 9. Pure Torsion [11, p. 235]

A fiber of circular cross section (radius *a*) is subject to a torsional moment M_t (Fig. 16). On a plane $z = \text{const.}$, the shear stress is resolved into two components,

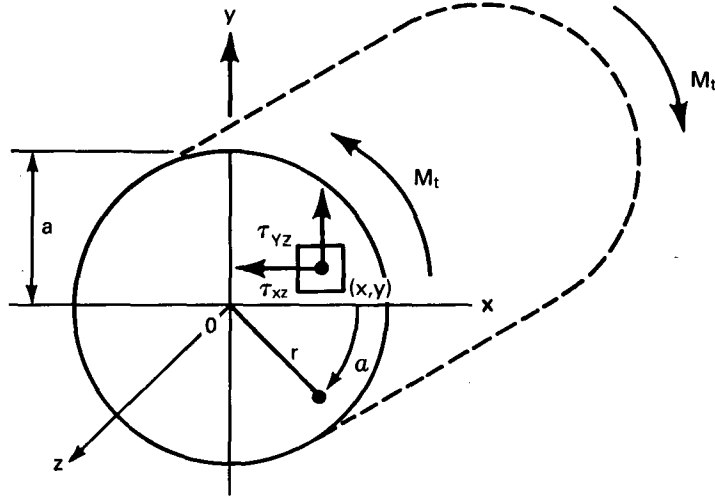


Fig. 16 — Fiber subject to pure torsion

$$\tau_{xz} = -\frac{2M_t y}{\pi a^4}$$

and

$$\tau_{yz} = \frac{2M_t x}{\pi a^4}$$

In polar coordinates r, α ,

$$\tau_{xz} = -\frac{2M_t r \sin \alpha}{\pi a^4}$$

and

$$\tau_{yz} = \frac{2M_t r \cos \alpha}{\pi a^4}$$

The combined shear is

$$\tau = (\tau_{xz}^2 + \tau_{yz}^2)^{1/2} = \frac{2M_t r}{\pi a^4}$$

and

$$\tau_{\max, r=a} = \frac{2M_t}{\pi a^3} = \frac{16 M_t}{\pi d^3}$$

The angle of twist per unit of length (β) is given by

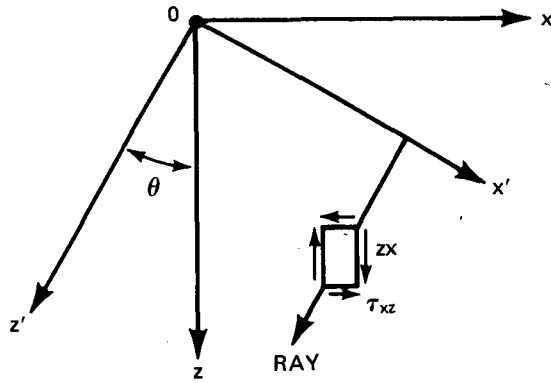
$$\beta = \frac{M_t}{GI_p} = \frac{32M_t}{G\pi d^4}$$

where G is the modulus of rigidity and I_p is the polar moment of inertia of the area of the cross section.

Assume that the optic ray is incident obliquely (at angle θ) to the cross sectional area parallel to the xz plane (Fig. 17). Resolve stress τ_{xz} into components parallel to and transverse to the ray. The only effective component is transverse:

$$p' = \sigma_{x'} = \tau_{xz} \sin 2\theta ; \quad q' = 0.$$

Fig. 17 — Oblique incidence in pure torsion



Next consider τ_{yz} . It has a pair τ_{zy} which lies in the xz plane (Fig. 18). The transverse component of $\tau_{z,y}$ is $\tau_{xy} = \tau_{zy} \sin \theta$. Thus, the secondary principal stresses at point (x,y) of the circular area of the cross section are

$$p' = \frac{\sigma_{x'}}{2} + \frac{1}{2} \sqrt{\sigma_{x'}^2 + 4\tau_{xy}^2}$$

and

$$q' = \frac{\sigma_{x'}}{2} - \frac{1}{2} \sqrt{\sigma_{x'}^2 + 4\tau_{xy}^2};$$

hence,

$$\begin{aligned} p' - q' &= 2 \sin \theta \sqrt{\tau_{xz}^2 \cos^2 \theta + \tau_{zy}^2} \\ &= 4 \sin \theta \frac{M_t}{\pi a^4} \sqrt{y^2 \cos^2 \theta + x^2} \\ &= \frac{4 \sin \theta M_t r}{\pi a^4} \sqrt{\sin^2 \alpha \cos^2 \theta + \cos^2 \alpha}. \end{aligned}$$

For fixed θ , this stress difference is maximized at $r = a$:

$$(p' - q')_{\max} = \frac{4 \sin \theta M_t}{\pi a^3} \sqrt{b^2 \sin^2 \alpha + \cos^2 \alpha}.$$

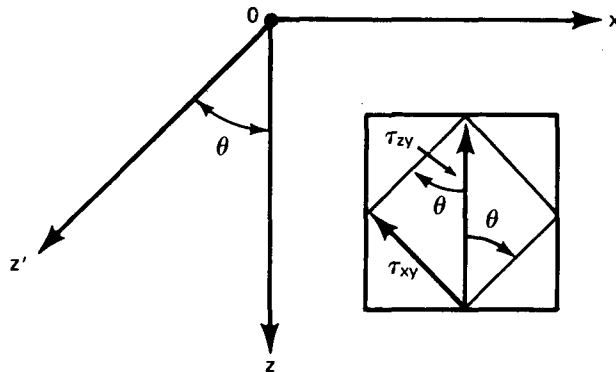


Fig. 18 — Oblique incidence with τ_{zy} component

When $x = 0$, namely when points are taken along the y axis,

$$p' - q' = \frac{4\sin \theta M_t}{\pi a^4} y \cos \theta$$

and

$$[(p' - q')_y]_{\max} = \frac{4\sin \theta M_t}{\pi a^3} \cos \theta = \frac{2M_t}{\pi a^3} \sin 2\theta.$$

When $y = 0$, namely for points along the x axis,

$$[(p' - q')_x]_{\max} = \frac{4\sin \theta M_t}{\pi a^3} = \frac{32\sin \theta M_t}{\pi d^3}$$

This case is computed numerically in the next section.

NUMERICAL CALCULATIONS

Stress-Optic Constant C

The theory of photoelasticity specifies the value of the stress-optic coefficient in terms of a *fringe value* f defined as follows:

Let m be the *fringe order* and $m\lambda$ the phase retardation, in units of wavelength, between the fast and slow waves in a birefringent material. Then the stress-optic law requires that

$$m\lambda = C(p - q)d.$$

Photoelasticians measure maximum shear stress $\tau_{\max} = \frac{p - q}{2}$. For convenience they define a *model fringe value* F by the relation

$$\tau_{\max} = \frac{p - q}{2} = mF,$$

from which it is seen that

$$F = \frac{\lambda}{2Cd}, \text{ or } C = \frac{\lambda}{2Fd}.$$

Thus,

$$m\lambda = \frac{\lambda}{2F} (p - q).$$

Here F is a material parameter whose value for a given material depends on the wavelength of the incident light and on the thickness. Usually values of F are tabulated for a standard thickness of 1 in. (25.4 mm). It is then called the *fringe value* f , the units of which are (lbs/in.²) \times inch/fringe (6.895 kPa \times 2.54 cm/fringe). For any other thickness (or propagation length),

$$F = \frac{f}{d} \quad (\text{units: psi/fringe or 6.895 kPa/fringe}).$$

Thus the fringe order is

$$m = \frac{(p - q)d}{2f} \quad (\text{units: fringe})$$

Now for every retardation (between slow and fast waves) of one wavelength the phase retardation is 2π rad. Hence, the total phase retardation in a fiber of length L is

$$\phi_d = m\lambda \times 2\pi = \frac{\pi(p-q)L}{f} \quad (\text{units: rad.})$$

(For consistent units p and q are in psi [6.895 kPa], L is in in. [2.54 cm].)

The value of f in the case of glass varies with the composition and wavelength. Frocht [12, p. 350] gives $f = 490$ to 1500 psi · in. (86 to 263 kPa · m) for a wavelength of $0.5461 \mu\text{m}$. Jessup [17] cites a value for glass in the range $f = 800$ psi · in. (140 kPa · m) upward.

A different approach to calculating C is adopted by physicists. They begin with

$$\Delta\phi_d = \frac{2\pi}{\lambda_0} m\lambda_0 = \frac{2\pi}{\lambda_0} C(p-q)d = k_0 C(p-q)d.$$

From this they define an effective difference in index of refraction Δn_{eff} between fast and slow rays caused by mechanical stress,

$$\Delta n_{\text{eff}} = C(p-q) \quad (\text{units: none}).$$

It is thus seen that the units of C are the inverse of the units of mechanical stress, namely $\text{m}^2 \text{N}^{-1}$. The quantity C is related to the classical stress-optical coefficients q_{ij} of a material. If the material is isotropic, then [6, p. 705]

$$\Delta n_{\text{eff}} = \frac{n_x^3}{2} (q_{11} - q_{12})(p-q) \quad (\text{units: none}).$$

Thus,

$$C = \frac{n_x^3}{2} (q_{11} - q_{12}) \quad \left(\text{units: } \frac{\text{m}^2}{\text{N}} \right).$$

Numerical values of q_{11} and q_{12} are usually derived from a knowledge of the strain-optic constants p_{ij} of the material. For stiffness tensors C_{jk} and compliance constants s_{ij} one has

$$p_{ij} = \sum_{k=1}^6 q_{ik} C_{jk}$$

and

$$q_{ij} = \sum_{k=1}^6 p_{ik} s_{jk}.$$

Since fused silica is elastically isotropic, one finds

$$p_{11} = q_{11} C_{11} + 2q_{12} C_{12}$$

and

$$p_{12} = q_{11} C_{12} + q_{12}(C_{11} + C_{12}).$$

Now, for fused silica, $n = 1.46$,

$$\left. \begin{aligned} C_{11} &= 7.85 \times 10^{10} \text{ N/m}^2 \\ C_{12} &= 1.61 \times 10^{10} \text{ N/m}^2 \end{aligned} \right\} \text{Ref. 18,}$$

and

$$\left. \begin{aligned} p_{11} &= 0.121 \\ p_{12} &= 0.270 \end{aligned} \right\} \text{Ref. 19.}$$

Solving by Cramer's rule, we obtain:

$$q_{11} = 3.98 \times 10^{-13} \text{ m}^2/\text{N} = 2.74 \times 10^{-9} \text{ in.}^2/\text{lb}$$

and

$$q_{12} = 2.78 \times 10^{-12} \text{ m}^2/\text{N} = 1.92 \times 10^{-8} \text{ in.}^2/\text{lb}.$$

Thus we estimate C to be

$$\begin{aligned} C &= \frac{1.46^3}{2} (2.74 \times 10^{-9} - 1.92 \times 10^{-8}) \\ &= -2.55 \times 10^{-8} \text{ in.}^2/\text{lb} = -3.70 \times 10^{-12} \text{ m}^2/\text{N}. \end{aligned}$$

We check this value by use of a formula from Frocht [12, p. 156]

$$C = \frac{\lambda}{2f} = \frac{5.461 \times 10^{-5}}{2 \times 1060} \approx 2.58 \times 10^{-8} \text{ in.}^2/\text{lb} (3.74 \times 10^{-12} \text{ m}^2/\text{N}).$$

The magnitude is close enough. Thus if we retain the units of λ in centimeters, take f to be 1060, and disregard the negative sign we see that our computed values of q_{11} and q_{12} are verified. An additional check on the value of C is found in [9], where C for fused silica is given as $-3.36 \times 10^{-12} \text{ m}^2/\text{N}$. This agrees closely with the values noted above from other sources.

We proceed now with the analysis of several cases of elastically stressed bodies.

Numerical Calculations of Fiber on a Mandrel (Case 6)

A fiber 80 μm in diameter with a cladding 55 μm in diameter and a core 4.5 μm in diameter is wound on a mandrel which is 1 cm in diameter. From the tension in the fiber T we wish to determine the difference in principal stresses in the core and the birefringent effect per unit complete turn.

We begin with an analysis of the loading. The relative areas are

$$A_{\text{TOT}} = \frac{\pi d^2}{4} = \frac{\pi}{4} \times (80 \times 10^{-6})^2 = 5.03 \times 10^3 \mu\text{m}^2 (7.79 \times 10^{-6} \text{ in.}^2),$$

$$A_{\text{cladding}} = \frac{\pi}{4} [(55 \times 10^{-6})^2 - (4.5 \times 10^{-6})^2] = 2.36 \times 10^3 \mu\text{m}^2 (3.66 \times 10^{-6} \text{ in.}^2),$$

$$A_{\text{core}} = \frac{\pi}{4} (4.5 \times 10^{-6})^2 = 15.9 \mu\text{m}^2 (2.47 \times 10^{-8} \text{ in.}^2),$$

and

$$A_{\text{substrate}} = 5.03 \times 10^3 - (2.36 \times 10^3 + 15.9) = 2.65 \times 10^3 \mu\text{m}^2 (4.105 \times 10^{-6} \text{ in.}^2).$$

Assume that a tension of 170 MPa (25,000 psi) is permitted. The tensile force on each area is

$$T_{\text{TOT}} = 25,000 \times 7.79 \times 10^{-6} = 0.195 \text{ lb} = 88.4 \text{ g} (0.867 \text{ N}),$$

$$T_{\text{cladding}} = \frac{3.66 \times 10^{-6}}{7.79 \times 10^{-6}} \times 0.1948 = 9.15 \times 10^{-2} \text{ lb} = 41.5 \text{ g} (0.407 \text{ N}),$$

$$T_{\text{core}} = \frac{2.47 \times 10^{-8}}{7.79 \times 10^{-6}} \times 0.1948 = 6.17 \times 10^{-4} \text{ lb} = 0.28 \text{ g} (2.74 \text{ mN}),$$

and

$$T_{\text{substrate}} = \frac{4.105 \times 10^{-6}}{7.79 \times 10^{-6}} \times 0.1948 = 1.03 \times 10^{-1} \text{ lb} = 46.6 \text{ g} (0.458 \text{ N}).$$

We now undertake a solution to the problem.

We know from Case 6 that the principal stresses are in the XY plane and the XZ plane:

$$(p - q)_{x,y} = 2 \left\{ \left[\frac{64yTr \sin^2 \frac{\phi}{2}}{\pi d^4} \right]^2 + \left[\frac{32}{3} \frac{T \sin \phi}{d^4} \left(\frac{d^2}{4} - y^2 \right) \right]^2 \right\}^{1/2}$$

and

$$(p - q)_{x,z} = 2 \left\{ \left[\frac{64yTr \sin^2 \frac{\phi}{2}}{\pi d^4} \right]^2 + \left[\frac{32}{3} y \frac{T \sin \phi}{d^4} \left(\frac{d^2}{4} - y^2 \right)^{1/2} \right]^2 \right\}^{1/2}$$

We consider $(p - q)_{x,y}$ first. Two approaches appear feasible in estimating the polarization effect of this quantity. In the first we consider the fiber to be homogeneous and subject it to a maximum tension T_{TOT} . We then calculate the principal stresses at $y = 4.5/2 = 2.25 \mu\text{m}$, for $d = 80 \mu\text{m}$. In the second approach we consider only the core and subject it to a tension T_{core} . The calculations are as follows. For component $(p - q)_{x,y}$: $T = T_{TOT}$, $d = 80 \mu\text{m}$, $y = 2.25 \mu\text{m}$, and $\phi = 90^\circ$. Then $d = 80 \times 10^{-6} \times 39.37 = 3.15 \times 10^{-3}$ in., $y = 2.25 \times 10^{-6} \times 39.37 = 8.86 \times 10^{-5}$ in., and

$$\begin{aligned} (p - q)_{x,y} &= 2T \left\{ \left[\frac{64 \times 8.86 \times 10^{-5} \times 1.97 \times 10^{-1} \times 0.5}{\pi (3.15 \times 10^{-3})^4} \right]^2 \right. \\ &\quad \left. + \left[\frac{32}{3} \times \frac{1}{(3.15 \times 10^{-3})^4} \left[\left(\frac{3.15 \times 10^{-3}}{2} \right)^2 - (8.85 \times 10^{-5})^2 \right] \right]^2 \right\}^{1/2} \\ &= 2T(3.26 \times 10^{12} + 7.22 \times 10^{10})^{1/2} \\ &= 3.65 \times 10^6 T \text{ psi, } T \text{ in lb (55.5 } T \text{ GPa, } T \text{ in kg, or 5.66 } T \text{ GPa, } T \text{ in N).} \end{aligned}$$

The secondary principal stresses at 4° inclination of the optic ray are

$$\begin{aligned} (p' - q')_{x,y} &= 3.65 \times 10^6 T \times \sin^2(4^\circ) \\ &= 1.776 \times 10^4 T \text{ psi, } T \text{ in lb (270 } T \text{ MPa, } T \text{ in kg, or 27.5 } T \text{ MPa, } T \text{ in N).} \end{aligned}$$

The total loading is $T_{TOT} = 0.1948$ lb (0.0884 kg or 0.867 N). Thus,

$$(p' - q')_{x,y} = 1.776 \times 10^4 \times 0.1948 = 3.46 \times 10^3 \text{ psi (23.9 MPa).}$$

Thus the difference Δn between slow and fast components is

$$\begin{aligned} \Delta n &= C[(p' - q')_{x,y}]_{\max} = -2.55 \times 10^{-8} \times 3.46 \times 10^3 \\ &= -8.83 \times 10^{-5}. \end{aligned}$$

Now assume $\phi = 180^\circ$; then

$$(p - q)_{x,y} = 2 \left[\frac{64 \times 8.86 \times 10^{-5} \times 1.97 \times 10^{-1} \times 1}{\pi (3.15 \times 10^{-3})^4} \right] T$$

and

$$= 7.22 \times 10^6 T \text{ psi, } T \text{ in lb (110 } T \text{ GPa, } T \text{ in kg, or 11.2 } T \text{ GPa, } T \text{ in N).}$$

The secondary principal stresses at 4° incidence of the optic ray to the fiber axis are

$$\begin{aligned}(p' - q')_{x,y} &= 7.22 \times 10^6 T \times \sin^2(4^\circ) \\ &= 3.51 \times 10^4 T \text{ psi, } T \text{ in lb (535 } T \text{ MPa, } T \text{ in kg, or } 54.6 T \text{ MPa, } T \text{ in N)}.\end{aligned}$$

Again let $T = T_{\text{TOT}} = 0.1948 \text{ lb (0.0884 kg or 0.867 N)}$. Then

$$(p' - q')_{x,y} = 3.51 \times 10^4 \times 0.1948 = 6.85 \times 10^3 \text{ psi (47.2 MPa)}.$$

Thus,

$$\Delta n = -2.55 \times 10^{-8} \times 6.85 \times 10^3 = -1.75 \times 10^{-4}.$$

Next, component $(p - q)_{x,z}$ is seen to be about the same as $(p - q)_{x,y}$. Hence, for $\phi = 180^\circ$, the total Δn is about $\sqrt{2}$ larger than for either component; i.e., $\Delta n = -1.75 \times 10^{-4} \times \sqrt{2} \approx -2.5 \times 10^{-4}$ at a tensile force $T = T_{\text{TOT}}$ which is close to the limit (that is, close to the ultimate stress of the glass fiber, taken here to be 170 MPa, or 25,000 psi).

Next, we make a calculation as if the core alone is wrapped on the mandrel.

Bare Core on a Mandrel (Case 6)

Let us consider only $(p - q)_{x,y}$, where

$$[(p - q)_{x,y}]_{\text{max}} = \frac{64}{\pi} \frac{T_r}{d^3}.$$

Using conventional units (T in lb, r and d in in.),

$$r = 0.5 \text{ cm} = 0.5/2.54 = 1.968 \times 10^{-1} \text{ in.}$$

and

$$d = 4.5 \mu\text{m} = 4.5 \times 10^{-6} \times 39.37 = 1.77 \times 10^{-4} \text{ in.},$$

thus

$$\begin{aligned}[(p - q)_{x,y}]_{\text{max}} &= \frac{64}{\pi} \frac{T \times 1.968 \times 10^{-1}}{(1.77 \times 10^{-4})^3} \\ &= 7.23 \times 10^{11} T \text{ psi, } T \text{ in lb (11.0 } T \text{ PPa, } T \text{ in kg, or } 1.12 T \text{ PPa, } T \text{ in N)}.\end{aligned}$$

The secondary stresses at 4° inclination of the optic ray are

$$\begin{aligned}[(p' - q')_{x,y}]_{\text{max}} &= 7.23 \times 10^{11} T \times \sin^2(4^\circ) \\ &= 3.51 \times 10^9 T \text{ psi, } T \text{ in lb (53.3 } T \text{ TPa, } T \text{ in kg, or } 5.44 T \text{ TPa, } T \text{ in N)}.\end{aligned}$$

Thus the increment in index of refraction is

$$\begin{aligned}\Delta n &= C[(p' - q')_{x,y}]_{\text{max}} = -2.55 \times 10^{-8} \times 3.51 \times 10^9 T \\ &= -89.7 T/\text{lb, } T \text{ in lb (-198 } T/\text{kg, } T \text{ in kg, or } 20.2 T/\text{N, } T \text{ in N)}.\end{aligned}$$

Let $T = T_{\text{core}} = 6.17 \times 10^{-4} \text{ lb (0.280 g or } 28.6 \mu\text{N)}$. Then

$$\Delta n = -89.7 \times 6.17 \times 10^{-4} = -5.53 \times 10^{-2}.$$

Parameter Variation for Calculations of Δn of a Bare Core on a Mandrel (Case 6)

(a) Let the parameter be the angle ζ between stress system and optic ray. The functional dependence of Δn on ζ is $\sin^2 \zeta$. Let $T = T_{\text{core}} = 6.17 \times 10^{-4} \text{ lb (0.280 g or } 2.74 \text{ mN)}$. Then the relationship between ζ and Δn is given in Table 1.

Table 1

ζ	Δn
0°	0
1°	-3.44×10^{-3}
2°	-1.37×10^{-2}
3°	-3.095×10^{-2}
4°	-5.5×10^{-2}

(b) Let the parameter be the tensile force $T = T_{\text{core}}$ at the ends of the fiber. Assume $\zeta = 4^\circ$ is the angle of incidence of the optic ray. Then the relationship between T and Δn is given in Table 2.

Table 2

T_{TOT} (lb)	T_{TOT} (g)	T_{TOT} (N)	T_{core} (lb)	T_{core} (g)	T_{core} (N)	Δn
1.947×10^{-2}	8.83	8.66×10^{-2}	6.17×10^{-5}	2.80×10^{-2}	2.74×10^{-4}	-5.5×10^{-3}
1.947×10^{-3}	8.83×10^{-1}	8.66×10^{-3}	6.17×10^{-6}	2.80×10^{-3}	2.74×10^{-5}	-5.5×10^{-4}
1.947×10^{-4}	8.83×10^{-2}	8.66×10^{-4}	6.17×10^{-7}	2.80×10^{-4}	2.74×10^{-6}	-5.5×10^{-5}
1.947×10^{-5}	8.83×10^{-3}	8.66×10^{-5}	6.17×10^{-8}	2.80×10^{-5}	2.74×10^{-7}	-5.5×10^{-6}

Fiber Squeezed by Diametral Press (Case 8)

The effective birefringent increment Δn is obtained from Case 8. We have

$$\begin{aligned} \Delta n &= C(p - q) = -2.55 \times 10^{-8} \text{ in.}^2/\text{lb} \times \frac{8}{\pi} \frac{P}{D} \frac{\text{lb}}{\text{in.}^2} \\ &= -6.50 \times 10^{-8} \frac{P}{D}. \end{aligned}$$

Suppose first that the force P acts on the core, $D = 4.5 \mu\text{m} = 1.77 \times 10^{-4} \text{ in.}$ Then

$$\Delta n = \frac{-6.50 \times 10^{-8}}{1.77 \times 10^{-4}} P = -3.67 \times 10^{-4} P.$$

To estimate P , assume that σ_y is the maximum allowable stress, say 170 MPa (25,000 psi). Then at the center of the fiber disk

$$|\sigma_y| = 170 \text{ MPa} = 25,000 \frac{\text{lb}}{\text{in.}^2} = \frac{6P}{\pi D}.$$

Thus,

$$P = \frac{\pi \times 1.77 \times 10^{-4} \text{ in.} \times 25,000 \text{ lb/in.}^2}{6} = 2.32 \text{ lb/in. (406 N/m)}.$$

The differential Δn due to birefringence is then

$$\Delta n = -3.67 \times 10^{-4} \times 2.32 = -8.5 \times 10^{-4}.$$

Average Δn Along a Horizontal Diameter (Case 8)

The stress $p - q$ can be averaged along a horizontal diameter by integration over the polar angle θ :

$$(p - q)_{AV} = \frac{4p}{\pi r} \int_0^{\pi/4} \frac{(\cos \theta - 2\cos \theta \sin^2 \theta) d\theta}{\pi/4}$$

$$\approx \frac{2.4 P}{\pi r} = \frac{4.8 P}{\pi D}$$

Hence, the differential Δn due to birefringence is

$$(\Delta n)_{AV} = -2.55 \times 10^{-8} \times \frac{4.8 \times 2.32}{\pi \times 1.77 \times 10^{-4}} = -5.1 \times 10^{-4}$$

Pure Torsion (Case 9)

Let us use the last formula of the analysis of Case 9 to find Δn . Now

$$(M_t)_{\max} = \frac{\pi d^3}{16} \tau_{\max}$$

Let $d = 80 \mu\text{m} = 3.15 \times 10^{-3}$ in., and assume

$$\begin{aligned} \tau_{\max} &= 2.8 \times 10^{-3} G = 2.8 \times 10^{-3} \times 4.5 \times 10^6 \\ &= 1.3 \times 10^4 \text{ psi (89.6 MPa)}. \end{aligned}$$

Here we have selected G for fused silica, and the factor 2.8×10^{-3} is the ratio of permissible tensile stress to Young's modulus. Thus

$$\begin{aligned} (M_t)_{\max} &= -\pi (3.15 \times 10^{-3})^3 \times 1.3 \times 10^4 / 16 \\ &\approx 7.98 \times 10^{-5} \text{ in lb.} \end{aligned}$$

Hence the maximum angle of twist per unit of length is

$$\begin{aligned} \beta_{\max} &= \frac{7.98 \times 10^{-5} \times 32}{4.5 \times 10^6 \times \pi \times (3.15 \times 10^{-3})^4} \\ &= \frac{1.83 \text{ rad}}{\text{in.}} = \frac{105^\circ}{\text{in.}} \left(\frac{0.72 \text{ rad}}{\text{cm}} \right). \end{aligned}$$

Now choose the angle of oblique incidence to be 4° . Then for a core which is $4.5 \mu\text{m}$ (1.77×10^{-4} in.) in diameter

$$\begin{aligned} (p' - q') &\approx \frac{4 \sin \theta M_t}{\pi a^3} \cdot \frac{x}{a} = \frac{4 \times \sin 4^\circ \times 7.98 \times 10^{-5} \text{ in-lb}}{\pi \left(\frac{3.15 \times 10^{-3}}{2} \right)^4} \frac{(1.77 \times 10^{-4})}{2} \\ &= 102 \text{ psi (703 kPa)}. \end{aligned}$$

Hence, finally, the differential Δn due to birefringence is

$$\Delta n = -2.55 \times 10^{-8} \times 102 = -2.60 \times 10^{-6}$$

We see that *pure* torsion has negligible birefringent effect for a fiber carrying a single mode. Twist, however, introduces coupled modes, even in a single mode fiber (see the section on coupled modes).

Fiber Subject to Random Stresses (Case 8)

Assume that the stress field in the fiber is randomly distributed and can be represented as having a *transverse* component of fluctuation,

$$\delta s_{\text{rms}} = \delta(p - q)_{\text{rms}}$$

Then the effective rms difference between the fast and slow components of birefringence is

$$\Delta n_{\text{rms}} = C \delta s_{\text{rms}}$$

From this one obtains the rms phase difference between the two components after a length L ,

$$\delta \phi_{\text{rms}} = k_0 \Delta n_{\text{rms}} L_{\text{eff}}, \quad L_{\text{eff}} \equiv \sqrt{2LL_c}$$

Our main interest is to calculate Δn_{rms} for fibers made of fused silica:

$$\Delta n_{\text{rms}} = -2.55 \times 10^{-8} \delta s_{\text{rms}} \quad (\delta s \text{ in psi})$$

$$[-3.70 \delta s_{\text{rms}} \quad (\delta s \text{ in TPa})].$$

We select for calculation a value of Δn_{rms} which is equal to that calculated for applied diametral forces, namely $\Delta n_{\text{rms}} = -8.5 \times 10^{-4}$. The corresponding fluctuation in stress required to generate an equal Δn is

$$\delta s_{\text{rms}} = \frac{-8.5 \times 10^{-4}}{-2.55 \times 10^{-8}} = 3.3 \times 10^4 \text{ psi (230 MPa)}$$

This is very large. We conclude that average frozen fluctuation stresses have negligible influence in producing a Δn of significance if they are of the order of 10^3 psi (7 MPa) or less. As an extreme case, suppose $\Delta n = 0.1 n = 0.146$. Then the required frozen stresses have magnitude

$$|\delta s_{\text{rms}}| = \frac{0.146}{2.55 \times 10^{-8}} = 5.7 \times 10^6 \text{ psi (39 GPa)}.$$

Such stresses are far beyond the ultimate strength of the fiber.

The phase difference after length L depends on L_c . Assume $\sqrt{2LL_c} \approx 1 \text{ m} = L_{\text{eff}}$. Then for $\Delta n = 8.5 \times 10^{-4}$ and $\lambda = 5.461 \times 10^{-7} \text{ m}$ we have

$$\delta \phi_{\text{rms}} = \frac{2\pi}{\lambda_0} \Delta n_{\text{rms}} L_{\text{eff}} = \frac{2\pi \times 8.5 \times 10^{-4}}{5.461 \times 10^{-7}} \times 1$$

$$= 9.78 \times 10^3 \text{ rad.}$$

If we desire $\delta \phi_{\text{rms}} = 1 \text{ rad}$, then $\delta s_{\text{rms}} \approx 3.4 \text{ psi (23 kPa)}$ and $\Delta n = 8.5 \times 10^{-8}$.

CONCLUSIONS

Laser light propagating in a fiber may experience a change in the state polarization when the fiber is subject to mechanical stress. The classical formula for this effect is written in terms of a retardation in units of wavelengths ($m\lambda_0$), or phase difference in units of radians ($\Delta\phi_d$) between slow and fast components of birefringence:

$$m\lambda = C(p - q)d$$

and

$$\Delta\phi_d = k_0 C(p - q)d$$

(symbols explained previously in text). An analysis of nine cases of applied stress has been presented. It is concluded that the birefringent effects are negligible in most applications because there are no components of stress transverse to the optic ray. Two important cases do show birefringent effects: fiber squeezed by diametral forces and fiber subject to random stresses. Numerical calculations predict that for fibers of fused silica, at the limit of allowable stress,

$$\Delta n_{\max} = -8.5 \times 10^{-4} \text{ for the case of applied diametral forces}$$

and

$$\Delta\phi_d \approx 1 \text{ rad if the rms stress fluctuation is 3.4 psi (23 kPa).}$$

The case of a fiber 80 μm in diameter with a core 4.5 μm in diameter wound on a mandrel 1 cm in diameter has also been numerically estimated for fused silica at the maximum allowable stress. Here the birefringent effect is negligible if the optic ray is parallel to the axis of the fiber. However if the optic ray is incident at 4° to the optic fiber, then it is estimated that

$$\Delta n_{\max} \approx -2.5 \times 10^{-4}.$$

REFERENCES

1. F.P. Kapron et al., "Birefringence in Dielectric Optical Waveguides," *IEEE J. Quantum Electron.* **QE8**, 222 (1972).
2. L.G. Cohen, "Measured Attenuation and Depolarization of Light Transmitted Along Glass Fibers," *Bell Syst. Tech. J.* **50**, 23 (1971).
3. A. Papp and H. Harms, "Polarization Optics of Index-Gradient Optical Waveguide Fibers," *Appl. Opt.* **14**, 2406 (1975).
4. H. Harms et al., "Magneto-optical Properties of Index-Gradient Optical Fibers," *Appl. Opt.* **15**, 799 (1976).
5. A.M. Smith, "Polarization and Magneto-optic Properties of Single-Mode Optical Fiber," *Appl. Opt.* **17**, 52 (1978).
6. M. Born and E. Wolf, *Principles of Optics*, 5th ed., Pergamon, New York, 1975.
7. R.C. Jones, "A New Calculus for the Treatment of Optical Systems," *J. Opt. Soc. Am.* **31**, 488 (1941).
8. G.N. Ramachandran and S. Ramaseshan, "Crystal Optics," in *Handbuch der Physik*, edited by S.F. Flügge, Springer-Verlag, Berlin, 1961, Vol. XXV/1, p. 1.
9. R. Ulrich and A. Simon, "Polarization Optics of Twisted Single Mode Fibers," *Appl. Opt.* **18**, 2241 (1979).
10. R. Ulrich, "Representation of Codirectional Coupled Waves," *Opt. Lett.* **1**, 109 (1977).
11. S. Timoshenko, *Theory of Elasticity*, 1st ed., McGraw-Hill, New York, 1934.
12. M.M. Frocht, *Photoelasticity*, Wiley, New York, 1941, Vol. I.
13. S. Timoshenko, *Strength of Materials*, 3rd ed., Van Nostrand, New York, 1955, Vol. I.

14. M.M. Frocht, *Photoelasticity*, Wiley, New York, 1948, Vol. II.
15. C.B. Biezeno and R. Grammel, *Engineering Dynamics*, Blackie, London, 1956, Vol. II, p. 107.
16. G.I. Taylor, Diffusion by Continuous Movements, Proc. London Math. Soc. **20**, 196 (1922).
17. H.T. Jessop, "Photoelasticity," in *Handbuch der Physik*, edited by S. Flügge, Springer-Verlag, Berlin, 1958, Vol. VI, p. 163.
18. B.A. Auld, *Acoustic Fields and Waves in Solids*, Wiley, New York, 1973, Vol. I, p. 369.
19. D.A. Pinnow, "Materials for Nonlinear Optics," in *Laser Handbook*, edited by F.T. Arecchi and E.O. Schulz-DuBois, North-Holland, Amsterdam, 1972, Vol. 1, p. 999.